



# Breakthroughs in medicine and bioimaging with up-conversion nanoparticles

This article was published in the following Dove Press journal:  
*International Journal of Nanomedicine*

Iman Rostami <sup>1,2</sup>  
Hamideh Rezvani Alanagh<sup>2</sup>  
Zhiyuan Hu<sup>2,3</sup>  
Sarah H Shahmoradian <sup>1</sup>

<sup>1</sup>Laboratory of Biomolecular Research, Department of Biology and Chemistry, Paul Scherrer Institute, Villigen, PSI 5232, Switzerland; <sup>2</sup>CAS Key Laboratory of Standardization and Measurement for Nanotechnology, CAS Key Laboratory for Biomedical Effects of Nanomaterials and Nanosafety, CAS Center for Excellence in Nanoscience, National Center for Nanoscience and Technology of China, Beijing 100190, People's Republic of China; <sup>3</sup>Center for Neuroscience Research, School of Basic Medical Sciences, Fujian Medical University, Fuzhou, Fujian Province 350108, People's Republic of China

**Abstract:** Nanomedicine is a medical application of biochemistry incorporated with materials chemistry at the scale of nanometer for the purpose of diagnosis, prevention, and treatment. New models and approaches are typically associated with nanomedicine for precise multifunctional diagnostic systems at molecular level. Hence, employing nanoparticles (NPs) has unveiled new opportunities for efficient therapies and remedy of difficult-to-cure diseases. Among all types of inorganic NPs, lanthanide-doped up-conversion nanoparticles (UCNPs) have shown excellent potential for biomedical applications, especially for multimodal bioimaging including fluorescence and electron microscopy. Association of these visualization techniques plus the capability for transporting biomaterials and drugs make them superior agents in the field of nanomedicine. Accordingly, in this review, we firstly presented a fundamental understanding of physical and optical properties of UCNPs and secondly, we illustrated some of the prominent associations with bioimaging, theranostics, cancer therapy, and optogenetics.

**Keywords:** up-conversion nanoparticles, bioimaging, theranostics, therapy

## Introduction

Nanomedicine is an interdisciplinary, preclinical research field that is a combination of nanotechnology and biochemistry which facilitates biomedical sciences for diagnosis and treatment at molecular scale.<sup>1</sup> The majority of biological processes which occur at nanoscale, might provide new models and standards for improving the medical profession.<sup>2</sup> Accordingly, the use of nanoscale materials is unveiling a new world of highly-sensitive treatments for hard-to-cure diseases, especially for the purpose of precise drug delivery, prophylactics, biosensing, and imaging.<sup>3</sup> Due to the unique properties of materials of this size, such as high chemical/heat resistance, modifying and transporting capability, optoelectronic properties, quantum behavior, and proper sizes against dimension of a multitude of biomaterials such as proteins and nucleic acids, this field might be extraordinarily beneficial in medicine.<sup>4</sup> One of the exclusive and practical properties of materials at nanoscale is their size-dependency that eventuates various fundamental behaviors such as luminescence, conductivity, chemical reactivity and magnetic permeability from particles as a function of the size.<sup>5,6</sup> Another distinctive property of materials at this scale is the high surface-area-to-volume ratio that provides a relatively large substrate for chemical or biomaterials' attachment.<sup>7</sup> Researchers have been able to modify such surfaces on nanoparticles (NPs) to generate fine platforms that involve coating molecules with active peripheral sides to make well-tuned particles

Correspondence: Iman Rostami  
Paul Scherrer Institute, OFLC/110,  
Forschungsstrasse 111, Villigen, PSI 5232,  
Switzerland  
Tel +41 56 310 3309  
Email [iman.rostami@psi.ch](mailto:iman.rostami@psi.ch)

for loading drugs.<sup>8</sup> The sum of all these properties enhances the efficacy of medical applications and diminishes the side effects and toxicity of these materials.<sup>9</sup> However, employing inorganic NPs, either for treatment or diagnostics, is not absolutely compatible in the human body and there are several side effects with inherent toxicity of these undersized objects. Therefore, providing NPs with lower toxicity, such as lanthanide-doped up-conversion nanoparticles (UCNPs) might enhance the potential of utilizing this class of probes in medicine.

Usually, numerous difficulties arise with conventional medical approaches for delivering drugs and efficient targeting. In some cases, the drug molecules have low water solubility, or they can be well-absorbed by the target but are removed from the body before sufficient effect to the cells and organelles to provide beneficial treatment.<sup>10</sup> Also, drugs with a higher effectiveness can possess a higher toxic profile that may lead to adverse effects and most notably cause damage to normal and healthy sites. This is a well-known phenomenon of the poor specificity of treatment agents to be taken up by the disease-affected tissues.<sup>11</sup> Nanomedicines, by contrast, provides assurance of sufficient drug loading to the body, by having a prolonged circulation time in the blood and by delivering the drug specifically to the areas where the treatment is needed.<sup>12</sup> This helps to maintain the required dose of drug in the body, and importantly, prevents salient damage to the healthy tissues that would otherwise be caused by the therapeutic drug molecules.<sup>13</sup> In addition, these therapeutic reagents that are transported using nanomaterials, have shown an increased loading of the drugs to the organs in the body compared with chemicals in classical delivery matrices.<sup>14</sup> Nanomedicine has also been approved by the US Food and Drug Administration (FDA) for the aid of diverse nanotechnology diagnostic approaches and nanodrugs.<sup>15,16</sup>

## NPs

NPs, due to their small sizes, customized surface, multi-functional capabilities, and water solubility, are creative agents for transporting biomaterials and drugs to site-specific emplacements.<sup>17</sup> The expansion of NPs in medicine has also led to further classes of clinical studies such as early diagnosis of pathologies, prediction and prevention using smart nanodevices.<sup>18</sup> NPs positively manipulate the enhanced permeability and retention (EPR) effect to reach the pathological tissues or intended area in the body through their quantum property.<sup>19</sup> After targeting the

tissue, cell penetration is the next challenging barrier for therapeutic effect of drugs which might be feasible with objects at nanoscale. Recent studies have demonstrated that the NPs less than 100 nm in size are able to pass through the cell membranes via endocytosis. Penetrability of cell membrane against NPs makes this important possible to reach the cell organelles such as the nucleus, lysosome, and mitochondrion.<sup>20,21</sup> Since different types of nanomaterials can be manufactured, ranging from carbon nanotubes, metal oxides NPs, polymeric NPs, dendrimers, quantum dots (QDs), and UCNPs (Figure 1), this might be a great advantage toward inventing more versatile diagnostic and treatment solutions for diseases such as different types of cancers, viral diseases, and neurodegenerative disorders.<sup>22–24</sup>

## Surface modification of NPs

A wide range of NPs exist with different properties and various precursors that demand mainstream attention. These materials might be organic such as semiconducting polymer dots, lipid drops, and nanosize carbon allotropes, or inorganic such as gold-, silver-, and lanthanide-doped NPs, rendering them particularly attractive as targeting and imaging reagents for biological specimens.<sup>25</sup> Nevertheless, NPs in the body act as a double-edged

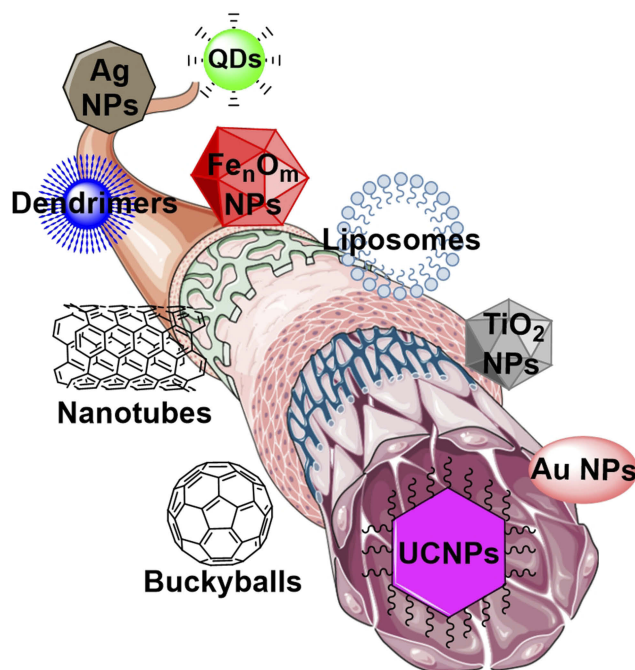


**Figure 1** Most commonly used nanomaterials in nanomedicine manufactured from different substances.

**Note:** The figure was produced by smart servier medical art library in combination with ChemDrew.

sword and despite their advantages, these small materials usually have inherent toxicity due to their sizes and potential to penetrate and accumulate in the main organs or bone marrow and generate new disorders.<sup>26</sup> This normally results in systemic toxicity and irreparable side effects; therefore, modification and functionalization of these particles with biocompatible molecules is being applied to convert them to low- or non-toxic objects with a safer result for diagnostics and therapeutics.<sup>27</sup>

Modification of NPs for drug delivery requires interdisciplinary approaches and heeding the physical and chemical properties of pertinent materials in addition to subsequent responses in the biological environment. In order to have efficacious drug delivery, the NPs need to possess enough stability for modification and capacity for loading desirable drug molecules, plus protecting drug bioactivity and boosting biocompatibility.<sup>28,29</sup>

Surface modification requires stable and appropriate NPs that might load the drugs or biomaterials without alterations in physicochemical of therapeutic agents; moreover, these materials should be able to release the drug after delivery to the intended diseased sites. A variety of common drug loading methods have been used for modification of NPs, including encapsulation, direct adsorption of the drugs via hydrophobic interaction or Van-der-Waals bonding, and chemical reactions such as covalent bonding between the active groups on the surface of NPs and functional groups on the scaffold of drugs and biomaterials.<sup>30</sup>

To develop noninvasive and impactful NPs, researchers, in the first step, attempt to coat them with biocompatible materials for therapeutic applications. Some of the most commonly used reagents are polyethylene glycol (PEG), succinic acid, thioglycolic acid, and silicon oxide that are loadable for biomaterials such as peptides, proteins, nucleic acids (e.g., DNA and RNA), and antibodies.<sup>31–33</sup> This layout turns out a platform for biolabels followed by selective targeting, and also provides a basis for binding the drugs and dyes on peripheral side of metal NPs.<sup>34</sup> PEG is a typical non-immunogenic organic compound with a linear or branched polyether terminated with hydroxyl (–OH) or the other functional groups such as amine (–NH<sub>2</sub>), carboxyl (–COOH) or thiol (–SH). The general configuration of PEG incorporation with a drug delivery system is shown in Figure 2 together with a schematic illustration of UCNPs conjugated PEG-based prodrug with the targeting agent.<sup>35</sup>

The PEG, in different sizes, has been used very routinely in various biological, chemical, and pharmaceutical

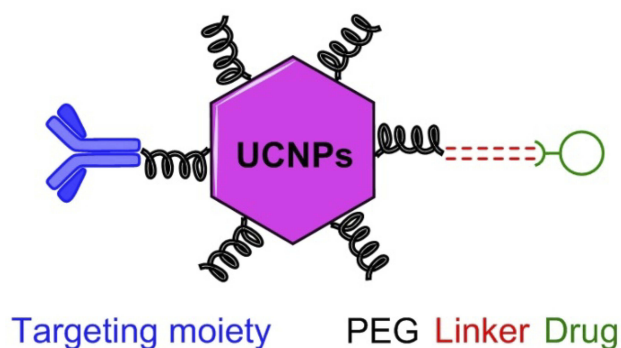


**Figure 2** Schematic presentation of UCNPs-PEG-based prodrug with targeting agent.

applications due to its low toxicity and reproducibility of results.<sup>36</sup> This compound gives higher water solubility to the proteins, drugs, and even inorganic NPs and also diminishes aggregation of complex, besides providing high flexibility for labeling tags and cross-linkers without steric hindrance. PEGs have also been used to functionalize the surface of NPs in combination with hydrophobic polymer to assemble amphiphilic diblock co-polymers. This method can generate plasmonic vesicles or dimers to improve drug delivery and enhance optical signals.<sup>37,38</sup>

## UCNPs

UCNPs are a class of luminescent nanomaterials that turn lower energy sources into higher energy luminescent emissions, which is a prodigious phenomenon in nonlinear optics.<sup>39</sup> These NPs, due to high fluorescence intensity under NIR irradiation and sufficient physical permanence, have been recently used for different demands, such as medical applications, new generations of printing, and even security of banknotes.<sup>40–49</sup> The up-conversion phenomenon was first proposed by Bloembergen in 1959, who suggested the detection of NIR light by electron transferring and counting the sequential absorption between electron shells or energy states of single ions.<sup>50</sup> This concept was then pursued by Auzel, and in 1966 he could explain high efficient up-conversion by electron transferring between energy states of two lanthanides (Yb<sup>3+</sup> and Er<sup>3+</sup>).<sup>51</sup> Figure 3 shows the general energy states diagram of the trivalent (tripositive) lanthanide ions doped in a low-symmetry crystal. The pointed lines in this figure represent practical up-conversion emissive excited layers that indicate the higher possibility of electron existence in these shells.<sup>52,53</sup>

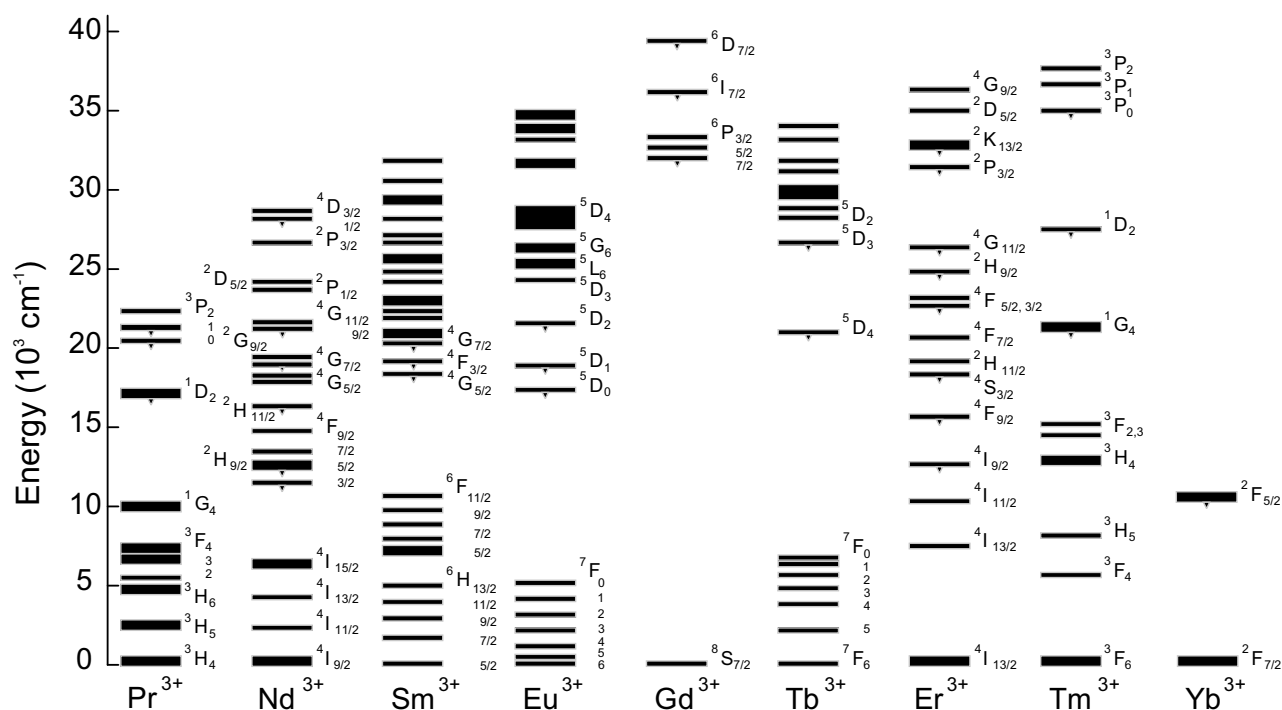


Figure 3 General energy states diagram of the lanthanide ions doped in a low-symmetry crystal.<sup>52,53</sup>

## Principle of lanthanides' luminescence

Lanthanide ions in solids are either divalent or trivalent with  $4f^n, 5s^2, 5p^6$  electron configuration with  $n=0-14$ . The electrons might be partly filled in  $4f$  orbitals by different arrangements and it can give rise to specific optical and magnetic properties for each configuration.<sup>54,55</sup> Since the electrons have a certain number of positions and orientations in available orbitals, the configuration possibility for electronic arrangement might take place within different levels of electron shells, and it can generate a wide range of energy values from NIR to ultraviolet (UV).<sup>56</sup> Principally, the most common valence states of the lanthanide ions in solids are the trivalent types, and doping the trivalent ions in different host lattices such as fluorides and oxides supplies stacks of absorption and emission wavelengths.<sup>57</sup> The independency of host lattices in this case and high yield energy transferring within the crystal lattice make the lanthanide ions suitable for spectral conversion and optical applications. The optical properties with these elements arise from luminescence phenomenon and electron transferring between allowed energy states as well as common fluorophores.<sup>58</sup> As a matter of fact, the up-conversion process follows anti-Stokes emission since longer wavelengths convert to shorter wavelengths, and in this system essentially, two NIR photons incorporate to produce one visible photon.<sup>59,60</sup>

To date, a plethora of studies have investigated and proved the mechanisms of up-conversion luminescence (UCL).<sup>61,62</sup> Principally, the long lifetime excited states of UCNPs affect the mechanism of the up-conversion energy transferring process and this has been developed different types of up-conversion mechanisms such as excited state absorption (ESA), up-conversion by energy transfer (ETU), two-photon absorption (TPA), cooperative sensitization up-conversion (CSU), cross-relaxation (CR), photon avalanche (PA), and energy migration-mediated up-conversion (EMU). Each of these mechanisms follows a specific pathway and they result in different efficiency in terms of luminescence output.<sup>53,63</sup>

## UCNPs' composition

UCNPs are composed of transparent inorganic crystals as host matrices that are co-doped with optical active trivalent lanthanide ions as the luminescent factors.<sup>64</sup> Luminescent lanthanide ions take place among the crystalline host matrices during the crystal lattice formation and the quantum yield (QY) of emissions (brightness) by these NPs is strongly dependent on the composition of substitutes within crystals.<sup>65,66</sup>

## Host matrix

Host matrices play important roles in governing optical properties and chemical/heat stability of UCNPs. Different host matrices have been used for UCNPs and each of them has a specific coordination number, certain energy transfer distance from the luminescent core, and specific output of energy transfer.<sup>67</sup> Therefore, it is crucial to choose an appropriate host matrix as frame for these NPs. Host matrices require several properties to better assist with energy transferring in UCNPs, such as high crystal and chemical stability to reduce degradation, low photon cut-off energy to reduce non-radiative relaxation, low chemical symmetry to enhance transition possibility, and high transparency to enhance transmission of NIR photons into the crystal lattice.<sup>68</sup> In general, the host matrices need close lattice matching with dopant ions and low resonance energy of lattice vibrations within the crystals. As all trivalent lanthanides ions expose homogeneous ionic size and identical chemical properties, their inorganic compounds are consummate for host matrices of up-converting lanthanide dopant ions. Thus far, multifarious host materials such as LiYF<sub>4</sub>, NaYF<sub>4</sub>, NaGdF<sub>4</sub>, NaLuF<sub>4</sub>, BaYF<sub>5</sub>, KY<sub>3</sub>F<sub>10</sub>, BaGdF<sub>5</sub>, SrF<sub>2</sub>, and BaF<sub>2</sub> have been developed and reviewed in various valuable articles.<sup>56,63,69,70</sup> Different host lattices can provide different crystal structures and different morphologies of the nanocrystals, and each of these factors can be effective in luminescence efficiency. For instance, the KLu<sub>2</sub>F<sub>7</sub> hexagonal-prism crystals, synthesized by controlling the ratio of F<sup>-</sup>/Ln<sup>3+</sup>, have shown optimal and higher UC emission intensity in comparison to the known β-NaREF<sub>4</sub> (RE=Y and Gd).<sup>71</sup> Nevertheless, the NaREF<sub>4</sub> family, due to the unique crystal composition and chemical stability among the series of host materials, has been utilized as the most popular host matrix for UCNPs' fabrication.<sup>72,73</sup> The cubic phase (α) and hexagonal phase (β) are two phases of this structure, and it has been frequently reported and proven that β-phase has higher luminescence efficiency than α-phase.<sup>74</sup>

## Sensitizers, activators, and energy mediators

An ideal sensitizer is able to improve the pumping efficiency of electrons to upper energy states of activators by having relatively high absorption cross-sections of NIR light and well-matched excited electron shells/energy states with the associated activator.<sup>75</sup> Yb<sup>3+</sup> might be a superior candidate for donating and transferring energy into the entire lanthanide-doped nanocrystal due to its

simple energy state configuration with large absorption cross-section (<sup>2</sup>F<sub>7/2</sub>-<sup>2</sup>F<sub>5/2</sub>). In Figure 3 the energy states diagram of the lanthanide ions illustrates that the electrons from the excited energy state of Yb<sup>3+</sup> (<sup>2</sup>F<sub>5/2</sub>) can transfer to excited states of Er<sup>3+</sup> and Tm<sup>3+</sup> due to close electron states.<sup>76</sup> Gd<sup>3+</sup>, due to having a big energy gap (<sup>6</sup>P<sub>7/2</sub>-<sup>8</sup>S<sub>7/2</sub>), can be a supreme energy mediator to immigrate the energy through the layers nanocrystal unit.<sup>77</sup>

Activators are responsible for generating and emitting the output fluorescence from the core of the UCNPs.<sup>78</sup> An ideal activator must possess numerous long-lived intermediate energy states. The ladder-like arrangement of these states might have an affirmative influence on the emission efficiency.<sup>62</sup> Excitation of electrons from the lowest state to the intermediate states of activators near the excited electron shells of sensitizers can elevate further transitions to the higher states. On the other hand, increasing the concentration of doped activators might quench the electron transmission of activators by non-radiative relaxation either within the same lanthanide or between two different elements with two pairs of electron shells with the same energy states.<sup>78,79</sup> According to these characteristics, Er<sup>3+</sup> and Tm<sup>3+</sup> are ideal activators for Yb<sup>3+</sup> doped UCNPs' construction.<sup>80,81</sup>

## UCNPs' configuration

As outlined earlier, the function of host materials is very crucial in the luminescence process of lanthanide ions. The crystalline structure of host materials improves the f-f electronic transitions within individual lanthanide ions through the disturbing of 4f wave functions, and this affects the energy exchange interactions between dopant ions in several ways.<sup>82,83</sup> The crystal structure and dopant concentration of sublattices might incorporate with the strength and direction of energy transferring through a particular interionic gap between dopant ions.<sup>41</sup> Well-defined concentration of lanthanide dopant ions is surrounded within the crystalline host matrices, besides, crystallization in the right spot might increase the efficiency of desirable energy transferring and photoluminescence.<sup>84</sup> In our previous work, we showed that optimized concentration of dopant ions might guarantee the highest efficiency of energy transferring and energy migration along the different layers of crystal lattice.<sup>85</sup> Tuning of the distances and junctions of lanthanide-doped ions within the crystal lattice might change the output of interior energy migration of NPs from the outer layer toward the inner layer.<sup>86</sup> This interior energy

migration is also dependent on host sub-materials and their lattices' structure and configurations.

The core-shell strategy may provide a controllable composition over dopant compartment that is substantially a self-sufficient system of either the host matrix or lanthanide dopants; therefore, it creates new opportunities to apply new dopant interactions and enhances the stability of NPs' structure and photoluminescence lifetime.<sup>87</sup> Oftentimes, incompatible dopant ions which are separately located in different or even the same layers of nanocrystals can eliminate energy transmission or CRs within the crystal lattice and consequently quench the luminescence process.<sup>88</sup>

Materials science has developed a wide variety of core-shell NP components that are a combination of different layers of dissimilar materials such as metals, polymers, and semiconductors. However, combination of most of these materials is not feasible in UCNP crystals due to chemical incompatibility and quenching the energy migration in quantum states.<sup>89</sup> In the core-shell UCNPs, typically a lanthanide fluoride-based lattice (e.g.,  $\text{YF}_4$ ,  $\text{LaF}_4$  and  $\text{NaYF}_4$ ) employs as the host for the framework of these NPs. The rational tuning between fluorides and doping ions in UCNPs can influence the photoluminescence emission intensity. Furthermore, the host matrix needs to provide low photon cut-off energy and vibration of energy to situate a high concentration of lanthanide dopant ions and produce homogeneous doping.<sup>88</sup>

Increasing the UCL efficiency and decreasing surface defects of up-conversion nanocrystals is crucial to improve their optical properties, and dense crystalline shell layers matched with the core of NPs lattices (epitaxial shells) can help to promote these factors (Figure 4A left structure).<sup>90</sup> In

addition, combination of discrete functional units on the top of the surface (non-epitaxial shells) is applicable to provide a platform for entrapping complex drugs and generating therapeutic opportunities for labeling, transporting, and light-activated therapy.<sup>91</sup> These core-shell coatings provide high photochemical stability and facilitate multi-shelled formations (Figure 4A right structure).<sup>92</sup> A crucial point for generating core-shell structures is getting a maximized radiative spectral conversion and transmission; however, there are a few possibilities to make radiative channels. Non-epitaxial core-shell coating might be with organic substances (e.g., polymers and molecules as surfactant) and/or inorganic substances (e.g.,  $\text{SiO}_2$  and  $\text{TiO}_2$ ).<sup>93</sup> To acquire a desired structure and to avoid non-radiative relaxations, the combination of epitaxial and non-epitaxial shell coatings might be utilized. Technically, the epitaxial core-shell NPs serve as the cores for non-epitaxial shell coatings.

The other concern when manufacturing core-shell structures for UCNPs is to avoid luminescence quenching by the effect of hydroxyl groups on the lanthanide-doped elements such as  $\text{Er}^{3+}$  and  $\text{Yb}^{3+}$ .<sup>94,95</sup> Su et al found out that surface quenching can be prevented by growing an epitaxial inert  $\text{NaYF}_4$  shell around a core-shell gadolinium sublattice UCNPs, as a result of boosting the excitation energy trapping by activator (Figure 4B).<sup>96</sup> This shell is able to make an optical active gap between sanitizers/activators and surface ligands and solvents to protect the luminescent output. The results from a study by Yi et al also indicated that  $\text{NaYF}_4$  shell could isolate the activator ions doped in the core from aqueous quencher and enhance the fluorescence efficiency of  $\text{NaYF}_4:\text{Yb,Er/Tm}$  NPs.<sup>97</sup> The same results have been demonstrated by Zhang

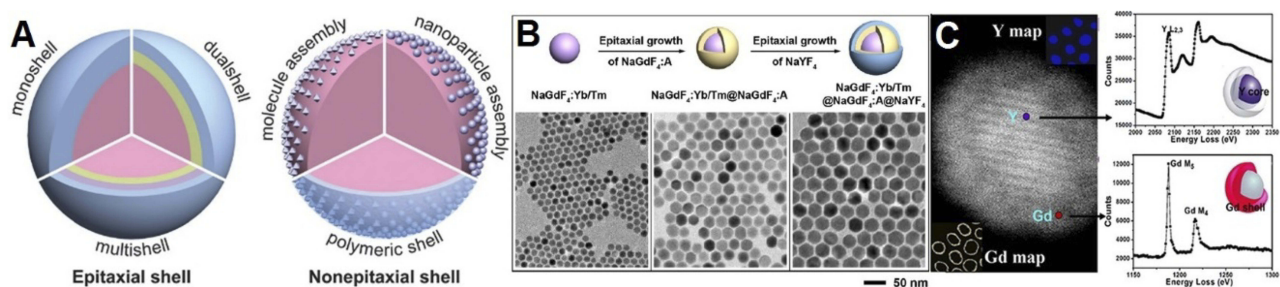


**Figure 4 (A)** Schematic illustrations of the typical structures of epitaxial and non-epitaxial shells for core-shell tuned UCNPs. Reproduced with permission from Chen X, Peng D, Ju Q, Wang F. Photon upconversion in core-shell nanoparticles. *Chem Soc Rev.* 2015;44(6):1318–1330.<sup>88</sup> Copyright the Royal Society of Chemistry 2015. **(B)** Schematic illustration of synthesizing and coating process for multilayer  $\text{NaYF}_4:\text{Yb,Tm}$  nanoparticles and TEM images from each step. Reproduced with permission from Su Q, Han S, Xie X, et al. The effect of surface coating on energy migration-mediated upconversion. *J Am Chem Soc.* 2012;134 (51):20849–20857.<sup>96</sup> Copyright American Chemistry Society 2012. **(C)** The left panel shows high-angle annular dark-field micrograph of a  $\text{NaYF}_4:\text{Yb,Er}/\text{NaGdF}_4$  nanoparticle with the chemical maps from the presence of yttrium (Y) in the core and gadolinium (Gd) in the shell of nanocrystal. The right panel shows the electron energy loss spectroscopy of Y and Gd edges from the nanoparticle with 2.4 nm shell. Reproduced with permission from Zhang F, Che R, Li X, et al. Direct imaging the upconversion nanocrystal core/shell structure at the subnanometer level: shell thickness dependence in upconverting optical properties. *Nano Lett.* 2012;12(6):2852–2858.<sup>98</sup> Copyright American Chemistry Society 2012.

et al for NaYF<sub>4</sub>:Yb,Er/NaGdF<sub>4</sub> core-shell NPs and the thickness of NaGdF<sub>4</sub> showed direct dependency on the optical response from the nanocrystals and resistance to quenching effects by aqueous solvents (Figure 4C).<sup>98</sup>

Even though using core-shell strategy could boost the luminescence efficiency of UCNPs, researchers have still been putting intemperate efforts into promoting the quantum yield (QY) of these NPs, especially for bioimaging proposes.<sup>99</sup> Developing the UCNPs with high QY might avoid the intense irradiation of NIR light to biological object that may overheat the tissues and/or cells. A recent report by Wisser et al represents an approach to remarkably enhance the up-conversion QY by conjugating a commercial fluorescence dye (ATTO 542) to the surface of UCNPs.<sup>100</sup> Efficient energy transferring happened between the organic dye and UCNP due to the equivalency in fluorescence energy band gap of the dye and the energy level of the activator (Er<sup>3+</sup>) from UCNP. The excited-state lifetime measurements indicated that the elevation of QY was related to the radiative rate gained by the conjugated dye. According to these results from the impact of emission sensitization, the dye-coated UCNPs showed better QY compared to the as-synthesized and ligand-stripped particles at different sizes.

## Synthesis of UCNPs

According to the literature, three common methods, so-called thermal decomposition, hydrothermal method, and non-hydrolytic colloidal method, have been utilized by scientists to synthesize UCNPs.<sup>101,102</sup> Several components are considered to get high luminescence efficiency and narrow size distributions of NPs with these methods, which are critical factors for high quality fabrication and various geometrical motifs.<sup>103</sup> Herein, we comprehensively discussed the two most common methods which have been utilized for synthesizing UCNPs with high UCL efficiency and homogeneous morphology of nanocrystals plus brief introductions on some other methods that are less utilized.

### Thermal decomposition method

Practically, thermal decomposition is a bottom-up synthesizing method that has become the most common strategy for synthesizing UCNPs.<sup>104</sup> This technique can produce uniform size/shape/phase NPs from nanoscaled building blocks. In terms of reaction time, it could be executed in a relatively shorter time, whilst, the organometallic complex precursors dissolve in high temperature (280–325°C) organic solvents containing stabilizing surfactants.

Oleylamine (OM), oleic acid (OA), and 1-octadecene (ODE) are typical surfactants with long chain primary alkylamine and polar end-capping groups.<sup>105</sup> The organic precursors commonly used are trifluoroacetate compounds. Much research has been dedicated to investigating the growth mechanisms of nanocrystals by optimizing different factors. Mai et al very comprehensively studied the growth mechanisms of different phases of up-conversion nanocrystals and their transition processed by conversional spectroscopy, transmission electron microscopy (TEM), and X-ray diffraction (XRD) techniques.<sup>106</sup>

The synthesis reaction in thermal decomposition generally includes four steps: i) nucleation in a delayed time, ii) particle growth by monomer supply, iii) size shrinkage by dissolution, and iv) aggregation. Figure 5A demonstrates schematic synthesis workflow for  $\alpha$ -NaYF<sub>4</sub>:Yb,Er UCNPs. The variety of reaction time, temperature, and concentration of reagents (organometallic compounds, surfactants, and solvents) provide various sizes, shapes, and also phases of NaYF<sub>4</sub>:Yb,Er UCNPs. Figure 5B–D shows different sizes of  $\beta$ -NaYF<sub>4</sub>-based NPs that have been synthesized under 330°C in OA/ODE for (Figure 5B) 15 min, (Figure 5C) 25 min, and (Figure 5D) 45 min.<sup>107</sup> Even though thermal decomposition method renders a low size distribution and homogeneity in shape of NPs, this approach still suffers some drawbacks for high quality output, for instance, requiring relatively high temperature under the reflux reaction with oxygen-free synthesis flask with inert gas infusion.<sup>108</sup> Furthermore, most of the synthesized NPs are fixed by surfactants, which are usually in contrast to biological applications and it causes non-biocompatible covers around the NPs, thus surface modification would be necessary.<sup>109</sup>

### Hydrothermal method

The hydrothermal method is a typical solution-based technique which has been used for synthesizing different types of nanocrystals.<sup>110</sup> The synthesis procedure can be relatively smoother than thermal decomposition in terms of temperature (130–240°C) and pressure. Nevertheless, the smoother synthesizing process suffers from a major drawback which is long reaction time depending on crystal growth and thermodynamic process.<sup>111,112</sup> In this method, unlike the thermal decomposition that mainly occurs in organic solvents, water-based media can be applied, and this moderate system allows some biocompatible chelating ligands such as sodium citrate and ethylene diamine tetra acetate (EDTA) cover the nanocrystals instead of long

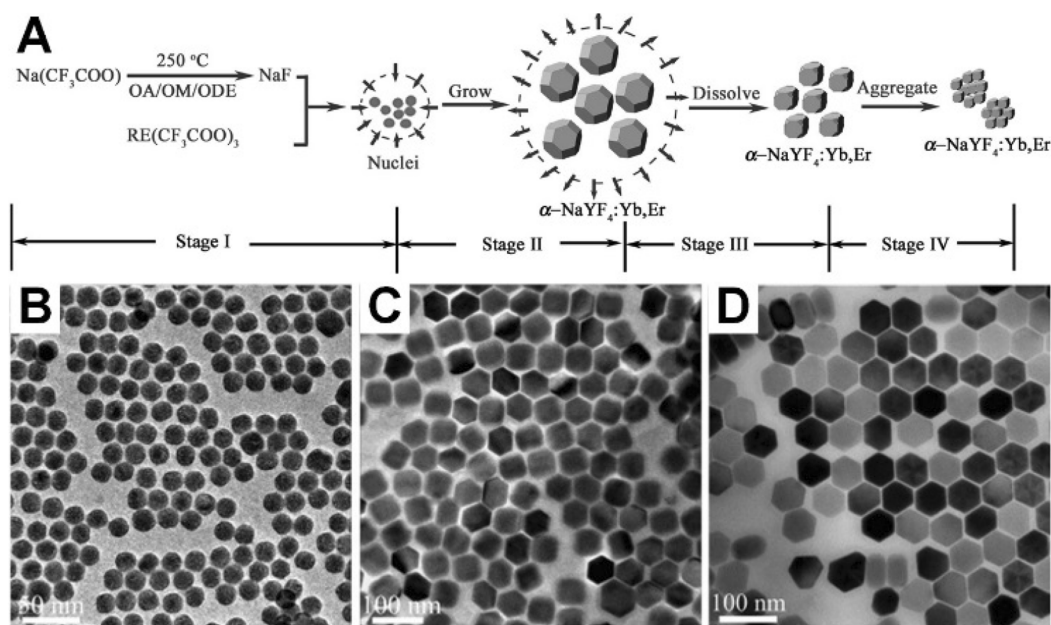


**Figure 5 (A)** Schematic procedure of synthesizing  $\alpha$ -NaYF<sub>4</sub>:Yb,Er nanocrystals and growing stages consecutively through the thermal decomposition method. Reproduced with permission from Mai H-X, Zhang Y-W, Sun L-D, Yan C-H. Size- and phase-controlled synthesis of monodisperse NaYF<sub>4</sub>:Yb,Er Nanocrystals from a unique delayed nucleation pathway monitored with upconversion spectroscopy. *J Phys Chem C*. 2007;111(37):13730–13739.<sup>106</sup> Copyright American Chemical Society 2007. Various sizes of NaYF<sub>4</sub>-based nanoparticles that have been synthesized under 330°C in OA/ODE (1/1) for (B) 15 min, (C) 25 min, and (D) 45 min. Reproduced with permission from Mai H-X, Zhang Y-W, Si R, et al. High-quality sodium rare-earth fluoride nanocrystals: controlled synthesis and optical properties. *J Am Chem Soc*. 2006;128(19):6426–6436.<sup>107</sup> Copyright American Chemical Society 2006.

chain non-biocompatible organic ligands.<sup>113,114</sup> Moreover, several studies have reported hydrothermal synthesizing in high temperatures and pressure reaction conditions.<sup>115–117</sup> It is likewise the thermal decomposition method that generates different morphologies and architectures by using and tuning different substances, solvents, and adjusting reaction time and temperature. Shen et al demonstrated that LaF<sub>3</sub>:Yb<sup>3+</sup>,RE<sup>3+</sup> (RE=Er and Tm) NPs prepared via a hydrothermal co-precipitation method, followed by heat treatment at 180°C, 400°C, and 600°C separately. This investigation showed that the UCL intensity and particle size of these NPs were enhanced by increasing heat treatment temperatures.<sup>117</sup> An elegant study by Zhang et al introduced a general solution-based hydrothermal technique for generation of well-controlled morphologies nanoarray crystals of sodium lanthanide fluorides. Green and blue fluorescences have been yielded from nanoarrays of NaYF<sub>4</sub> co-doped with Yb<sup>3+</sup> as sensitizer and Er<sup>3+</sup> and Tm<sup>3+</sup>, respectively, as the activators. These nanoarrays could propose superior potential as light sources for a new generation of solid-state lasers due to specific luminescence outputs and chemical flexibilities.<sup>118</sup>

Lately, great efforts have been put into new approaches for synthesizing UCNPs to make the process faster, cheaper, and more efficient, not only for fundamental

research, but also for high-tech applications.<sup>41,119–121</sup> Shao et al reported a fast and novel ion-exchange approach for synthesizing monodisperse  $\beta$ -NaYF<sub>4</sub> micro/nanocrystals at 50°C. In this approach, the size of the crystals was adjusted according to the pH value. The results from this work indicated that by monotonously increasing the pH value the size of production reduced with no evident changes in morphology and monodispersity.<sup>122</sup> Lei et al also reported a super facile approach for synthesizing of hexagonal phase NaBiF<sub>4</sub>:Yb<sup>3+</sup>, Ln<sup>3+</sup> (Ln=Er, Tm and Ho) UCNPs at room temperature. The replacement of bismuth (Bi) species instead of traditional host matrixes has made this method enormously economical. In the sense of energy efficiency for high volume fabrication of UCNPs, working in ambient and short time production is a substantial convenience which this approach might make it feasible.<sup>123</sup> The other approach for synthesizing UCNPs is polyol-mediated which is normally utilized for metal oxide particles such as Cu<sub>2</sub>O, SiO<sub>2</sub>, and TiO<sub>2</sub> etc.<sup>124,125</sup> This technique is a high boiling points method that can produce NPs with high dispersity in water. Glycol, diethylene glycol, and glycerol are three common polyols that can guarantee the stability of particles, control the particle growth, and prevent the agglomeration during and after the synthesis procedure.<sup>126</sup>



## UCNPs in medicine

UCNPs have recently attracted much attention in medicine due to numerous exclusivities that can ease diagnostic and therapeutic approaches. Higher detection sensitivity, broader signal dynamic ranges for biomarkers, and prediction of therapeutic responses are a few examples of positive contributions of these nanomaterials to medicine. UCNPs may be employed as multiplexed and sensitive nanobiomarkers with great ability to be excited in the tissue by infrared light instead of ultraviolet or visible lights to create photoluminescence emissions in a visible range.<sup>127</sup> Several advantages possessed by these NPs in biomedicine including capability for cell penetration due to their size (20–50 nm), high stability for surface modification, fine emission line widths (10–20 nm) compared with QDs (20–40 nm) and organic dyes (30–50 nm), and most importantly, low inherent toxicity.<sup>128,129</sup> The combination of these properties makes UCNPs extremely practical in medicine, especially for cancer therapy.<sup>130</sup>

Biocompatibility of UCNPs has been investigated with multiple functionalization and conditions.<sup>131–139</sup> Here, we have summarized and listed recent efforts to study their toxicities *in vitro* (Table 1). As previously established, these NPs do not have significant toxicity; however, coating and different functionalities have been used to tune their interactions with cells. Our unpublished experimental encounter with UCNPs (size =35 nm, time =2 h, 8 h, and 24 h, concentration =10 µg/mL, 50 µg/mL, and 100 µg/mL, assay = resazurin) also showed their low toxicity profiles.

The unique photoactivity of UCNPs makes them a potential NIR adjuster probe that has attracted extensive attention in the past decade in the context of materials sciences. Forasmuch as the UCNPs have ability to be remotely utilized in regulated photodynamic inactivation and photo-triggered release systems, these materials exhibit superior potential for image-guided therapy and therapeutic studies.<sup>140</sup>

Light, due to its easy handling and remote controlling capability, has been widely used as an external stimulus to affect photochemical reactions. Using UV and/or visible lights exhibit a variety of impediments based on the substantial high photon energy, such as material decomposition and low penetration into the tissue. In contrast, NIR light, with lower photon energy, renders less photo damage and higher penetration inside tissue.<sup>141</sup> The capability of UCNPs to turn NIR light to short-wavelength photons enables using low energy wavelength for photochemical reactions. Moreover, UCNPs, due to containing 4f electron

orbital states of lanthanide ions, provide rich optoelectronic and magnetic properties.<sup>142</sup> Therefore, UCNPs have been explored for single-mode luminescence imaging as beam absorbent in several techniques such as magnetic resonance imaging (MRI), X-ray computed tomography (CT), positron emission tomography (PET), and single photon emission computed tomography (SPECT). In particular, UCL imaging has drawn remarkably increased attention in clinical studies of neurodegenerative diseases.<sup>143,144</sup>

There are a number of benefits and limitations of each bioimaging technique and the fact that any single imaging technique is not able to fulfill all of the requirements in a completed determination; accordingly, it would be appropriate to perform a series of modulation imaging to compensate for all the needs of visualization. Each imaging modality has unique characteristics and properties in terms of anatomical information. Different properties of these techniques such as sensitivity, depth of penetration, tissue discrimination, spatial resolution, and image properties (2D and 3D) can offer applicable monitoring of the biodistribution and location of UCNPs in animals' bodies for therapy.<sup>145,146</sup> There is increasing consideration about supplementing imaging techniques by combining different instrumental methodologies to compensate for the weakness of each technique individually. Hence, it is essential to employ a particular imaging contrast agent for each bioimaging strategy, utilizing a multifunctional contrast agent might be ideal to prevent injections of several agents into the body and reduce side effects by exterior reagents.<sup>147,148</sup> Therefore, it might be practicable to create versatile UCNPs for bioimaging due to their unique physical and optical properties, such as containing high electron dense materials and positive signal enhancement which make them usable for electron microscopy, MRI, X-ray tomography and PET, and also multivalent targeting capability which converts them into appropriate cargos for drug delivery.<sup>149,150</sup>

## Applications in optical imaging

Optical imaging is a prominent and widely used tool in biological and clinical research due to its capability for visualizing the morphology and structure of cells (*in vitro*) and sub-cellular organelles (*in vivo*). The application of UCNPs can be extremely advantageous in cellular targeting, drug delivery to living objectives, fluorescence resonance energy transfer (FRET),<sup>151</sup> and for other purposes through surface conjugation of organic or biological molecules to generate various functional imaging probes. Zijlmans's lab used up-converting phosphor particles

Table 1 Experimental cell viability results of UCNPs under different conditions

NPs types	Coating layer	NPs size/ nm	Concentration	Cell types	Exp. time	Toxicity assay	Results [Ref.]
$\beta$ -NaYF <sub>4</sub> :TmYb/ NaYF <sub>4</sub>	Mesoporous silica, PEG and folic acid coating	92	300 $\mu$ g/mL	HeLa cells	24 h	CellTiter-Glo luminescent cell viability assay	No significant decrease in cell viability. <sup>131</sup>
NaYbF <sub>4</sub> :Er	Mesoporous silica	76	21.2 $\mu$ M	HeLa cells	12 h	CCK-8	Viability $\approx$ 90% cell. <sup>132</sup>
NaYF <sub>4</sub> :Yb,Er	PEG-oleate bilayer	25	75 $\mu$ g/mL	HAEC	24 h	MTT	Viability $\approx$ 50% cell. <sup>133</sup>
NaYF <sub>4</sub> :Yb,Er and NaYF <sub>4</sub> :Yb,Tm	Thin amine- terminated silica layer	54, 30, 20	750 $\mu$ g/mL	FAR-positive KB carcinoma cells	1 h	Light controlled cytotoxicity	No significant decrease in viability of cells in the presence or absence of any exposure to light excitation. <sup>134</sup>
NaYF <sub>4</sub> :Yb,Er	Different coating	Different sizes	62.5–125 $\mu$ g/mL	Dermal fibroblasts and human epidermal linear keratinocytes (HaCaT)	24 h	MTT test and optical microscopy	The fibroblast viability was not compromised by UCNPs and the viability of HaCaT cells varied from 52% to 100% based on the surface coating. <sup>136</sup>
NaGdF <sub>4</sub> :Yb,Er	PEG SiO <sub>2</sub> and SiO <sub>2</sub> -NH <sub>2</sub>	Different sizes: 225–379	2–50 $\mu$ g/mL	NIH3T3 and RAW264.7 cells	24–48 h	Cell culture viability (MTS), proliferation and apoptosis	No significant toxicity by modified NPs. <sup>137</sup>
NaGdF <sub>4</sub> :Yb,Er:Fe	SiO <sub>2</sub>	20 nm	1000 $\mu$ g/mL	Human cervical carcinoma cell line HeLa	24 h	MTT	Low cellular toxicity. Cellular viability was estimated to be greater than 89% after 24 h. <sup>138</sup>
BaGdF <sub>4</sub> :Yb,Er	Glycerol	93 nm (7%) and 178 nm (92%).	10, 50 and 100 mg/L	1321NI cells	1–3 h	The MTT Cell, the MTS cell viability assay, Neutral Red assay	No significant toxicity to human brain cells. <sup>139</sup>

conjugated with NeutrAvidin for detection of specific antigens in tissue sections or on cell membranes in 1999.<sup>152</sup> Recently, in similar work, Wu et al showed that UCNPs, with no on/off emission alteration, can be coated with amphiphilic biocompatible polymers. This study proved that the excitation of these materials with a modest-power continuous wave laser for optical microscopy investigation might provide strong UCL with low anti-Stokes autofluorescence, which is the ideal invention for single-molecule imaging (Figure 6A and B).<sup>153</sup> Recently, Vaithyanathan et al designed a fluorescent microscopy-based microfluidic trapping array for simultaneously interrogate single-cell responses.<sup>154</sup> In this work, two different lanthanides ( $\text{Eu}^{3+}$  and  $\text{Tb}^{3+}$ )-doped  $\text{NaYF}_4$  based NPs were employed to eliminate spectral overlap between tracking dyes and general fluorophores/biochemical stains. The fluorescent microscopy images from four different droplet subpopulations were: i) droplets with  $\text{Eu}^{3+}$ -doped NPs, ii) droplets with green protein fluorescence (GFP)-expressing HeLa cell, iii) droplets with co-encapsulation of NPs and GFP-expressing cell, and iv) empty droplets (Figure 6C). Nevertheless, there is an unanswered question associated with the optical distance between the light source and the objective tissue or cell due to complexity of tissue scattering and absorption. Pominova et al have theoretically studied this topic on bioimaging by employing UCNPs.<sup>155</sup> In this study, optimal distance between two optical fibers, one at the position of laser source and the second at receiving point of biological tissue, was measured. This simulation by Monte Carlo modeling could calculate the intensity ratio of the UCNPs' luminescence at different depths inside phantoms of biological tissues.

## Applications in cancer therapy

Employing light in medicine has a long history and it has been applied in many ancient cultures such as Greek, Egyptian, and Chinese for treatment of skin disorders, acne vulgaris, and eczema. A medical researcher in 1900, while conducting his study on the effect of an aromatic compound (acridine) on single-celled microorganisms, found that association of light with this fluorophore has a lethal effect on the cells.<sup>156</sup> This study discovered that the fluorescence output from the combination of acridine and light induced toxicity in the microorganisms. Later on, Tappeiner et al used this method in 1903 for the same purpose. They employed another type of fluorescent (eosin) using white light for skin tumor treatment and indicated it with photodynamic action phrase.<sup>157</sup> Since then, photodynamic therapy (PDT) has been investigated by researchers and medical specialties as an inoffensive approach in therapy, and fluorophores such as hematoporphyrin and coproporphyrin could improve the impact of PDT.<sup>158–160</sup> Photosensitizers such as photofrin are also being used in PDT for different types of cancer therapy. In principle, in PDT, a source of light with certain wavelength and energy irradiates a photosensitizer and transfers the energy from ground state to excited state.<sup>161</sup> When energy is released from higher energy states, it may be transferred to the adjacent oxygen and produce oxygenated products (e.g.,  $^1\text{O}_2$ ).<sup>162</sup> These reactive products with oxidative effects can progress inflammatory diseases and properly kill the cells.<sup>163</sup> In recent years, PDT has become an acceptable and prevalent technique as a cancer therapeutic method due to lower systemic toxicity for normal tissue and better selectivity for the tumor with fewer side effects in comparison with chemotherapy, radiation, and proton therapy.<sup>164</sup> Some NPs, such as QDs, gold nanomaterials, and polymers have been

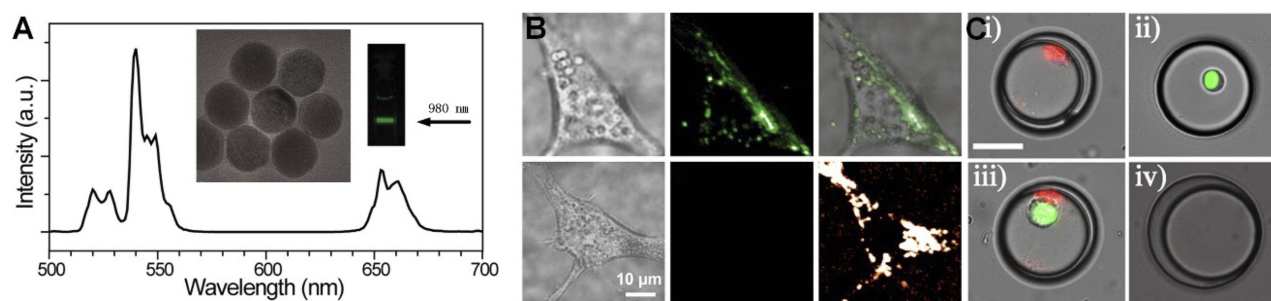


**Figure 6** (A) Luminescence spectrum of the UCNPs excited at 980 nm and TEM image of the UCNPs. (B) Cell imaging using UCNPs (top left) brightfield image of a cell with internalized UCNPs, (top middle) fluorescence imaging of stained cell with UCNPs excited at 980 nm, and (top right) merged. (Bottom left) brightfield image of a cell without UCNPs, (bottom middle) fluorescence imaging of cell without UCNPs, and (bottom right) cellular autofluorescence excited at 532 nm. (A, B) Reproduced from Wu S, Han G, Milliron DJ, et al. Non-blinking and photostable upconverted luminescence from single lanthanide-doped nanocrystals. *Proc Natl Acad Sci*. 2009;106(27):10917–10921.<sup>153</sup> (C) The fluorescent microscopy images from the trapped droplets by microfluidic array involving: i) droplets with lanthanide-doped NPs, ii) droplets with GFP-expressing cell, iii) droplets with co-encapsulated NPs and GFP-expressing cell, and iv) empty droplets. Reprinted by permission from Springer Nature: *Anal Bioanal Chem*, Luminescent nanomaterials for droplet tracking in a microfluidic trapping array, Vaithyanathan M, R Bajirani K, Darapaneni P, Safa N, Dorman JA, Melvin AT, Copyright 2019, doi:10.1007/s00216-018-1448-1.<sup>154</sup>

employed in PDT; however, most of these NPs turn short wavelengths into long wavelengths, which is called down-conversion luminescence, and this mechanism needs a higher energy density to activate photosensitizers.<sup>165</sup> Moreover, the higher energy lights can penetrate less into the tissue than lower energy lights and it brings difficulties to deep tissue imaging.<sup>166</sup> Therefore, a better solution for high PDT efficiency with fewer side effects is needed to employ this technique for further biomedical applications.<sup>167</sup> The use of UCNPs in PDT can cover a multitude of requirements as a result of deeper penetration of NIR light into the body, higher stability, and relatively easy surface modification. These materials in PDT usually require pre-coating with a shell which serves as a doping stage for photosensitizers, a probe platform for specific targeting, and UCNPs' stabilization. The  $\text{NaYF}_4:\text{Yb,Er}$  is one of the most commonly used UCNP types in PDT due to its high UCL efficiency.<sup>168,169</sup>

A multidisciplinary work by Zhao et al demonstrated the capability of UCNPs ( $\text{NaYF}_4:\text{Yb,Tm}$ ) for PDT and, simultaneously, it is a desirable platform for siRNA which may offer a major strategy in cancer therapy with superlative efficacy.<sup>170</sup> In this study, UCNPs were encapsulated with cationic conjugated polyelectrolyte brush (CCPEB). The richness of positive charges and photosensitizer behavior of this compound make it suitable for integrating the siRNA and the photosensitizer in a single molecule. The UCNPs coated with CCPEB showed efficacious PDT by producing  $^1\text{O}_2$ , and turning the photo-responsive cationic side-chains of CCPEB into zwitterionic chains could accelerate the siRNA releasing up to 80% at pH 5.0 under 1 hr NIR irradiation. Figure 7 shows a schematic illustration of UCNPs@CCPEB/siRNA fabrication and photosensitization process under 980 nm laser irradiation. The combination of PDT and

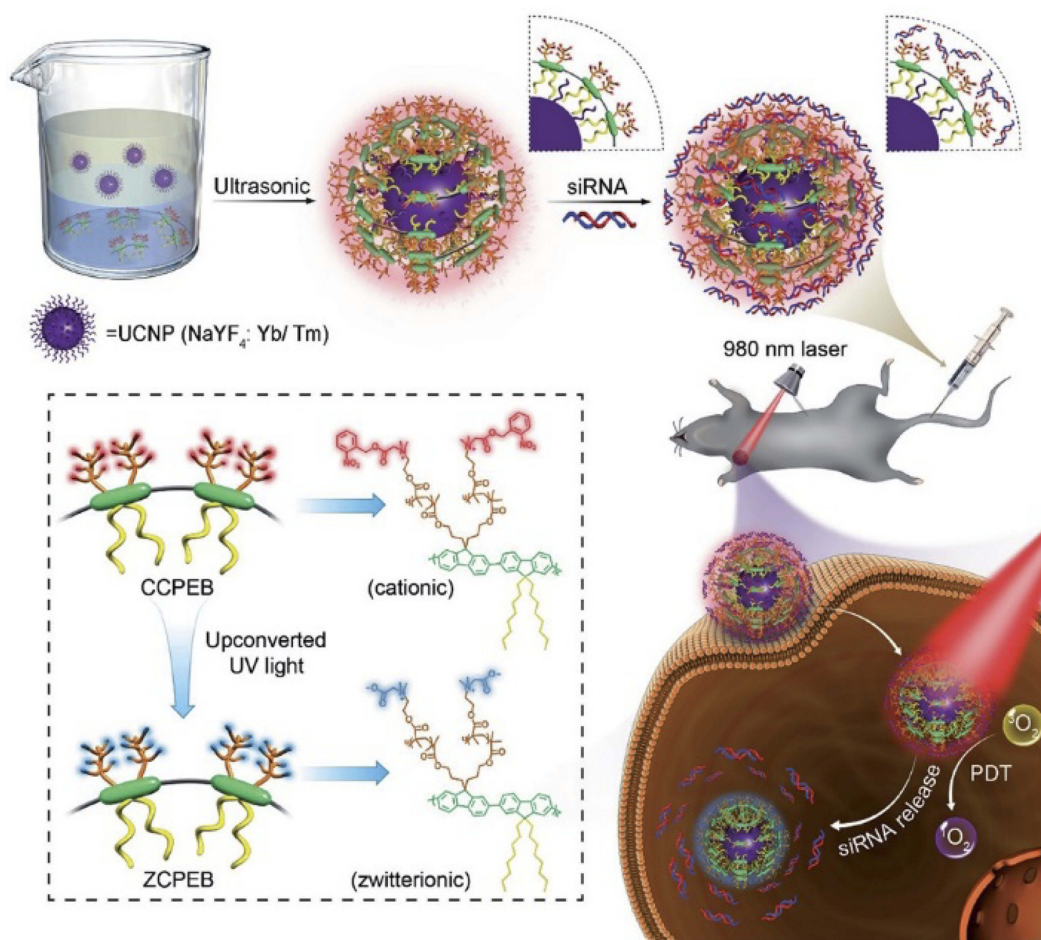


**Figure 7** The top scheme indicates fabrication of UCNPs@CCPEB and loading the siRNA process. The bottom scheme indicates the procedure of releasing the siRNA and PDT simultaneously under NIR excitation and UV/visible emission from UCNPs. Reproduced with permission from Zhao H, Hu W, Ma H, et al. Photo-induced charge-variable conjugated polyelectrolyte brushes encapsulating upconversion nanoparticles for promoted siRNA release and collaborative photodynamic therapy under NIR light irradiation. Reproduced from Zhao H, Hu W, Ma H, et al. Photo-induced charge-variable conjugated polyelectrolyte brushes encapsulating upconversion nanoparticles for promoted siRNA release and collaborative photodynamic therapy under NIR light irradiation. *Adv Funct Mater.* 2017;27(44):1702592<sup>170</sup> Copyright John Wiley and Sons.

siRNA therapy on tumor-bearing mice showed notable therapeutic potential for cancer treatment. Liu et al also created a novel nanovehicle by coating the UCNP with polydopamine (PDA). This complex is able to load indocyanine green (ICG), which can be triggered and heated by an 800–810 nm laser to overheat the tumor without damaging the surrounding tissue.<sup>171</sup>

Zhou et al illustrated a multiplexed simultaneous in situ technique for diagnostics of different biomarkers in intact tumor specimens by using single-band UCNP with different emissions that could provide a sensitive quantification of protein targeting. In this work, UCNP were modified with a silicon dioxide (SiO<sub>2</sub>) layer containing organic dyes to create a selective nanofilter around the nanocrystals and remove unwanted emission bands (Figure 8A).<sup>172</sup> UCNP covered with silicon dioxide layer in another study by Min et al, could provide a promising and innovative platform for remote controlling of light activation of a specific antitumor platinum prodrug by using an apoptosis sensing peptide (Figure 8B).<sup>173</sup> Several studies have shown that nucleic acids,<sup>174</sup> antibody-,<sup>175</sup> or peptide-conjugated<sup>176</sup> UCNP can be used to accomplish accurate molecular profiling and binding to protein targets in biodetections with high affinity and superior cell penetration.<sup>177,178</sup>

The use of surface-modified UCNP in animal experiments, chiefly in cancer research, for the purpose of drug delivery, bioimaging, and phototherapy has revealed reliable approaches for therapeutic innovations; however, there is an essential question about the statement and elimination of these particles from the body.<sup>179–182</sup> Liu et al reported an

inclusive study using PEG-modified NaGdF<sub>4</sub>:Yb,Er NPs for tumor targeting and in vivo imaging. The PEG was bearing maleimide on one side for attaching to a commercially available antitumor antibody and two phosphate groups on the other side for conjugating to the NP. One of the concerns in this study was pharmacokinetic interrogation on particle size-dependent biodistribution in mouse body and clearance pathways.<sup>183</sup> Three different sizes (5.1, 18.5, and 24.6 nm) of NPs were utilized for the output of post-injection examinations. The results from time-series in vivo experiments indicated major accumulation of these materials in liver and spleen, apart from the tumor. The clearance pathways investigation for NPs in this work showed the size dependency of elimination mechanism. Lower presence of smaller NPs in the liver and spleen at different time points post-injection, and also blood half-time calculation may prove that the smaller particles (5.1 nm) might have faster elimination from the renal pathway. The feces analysis showed that the biliary pathway could go forward with both big and small particle samples.

An innovative study by Ai et al has shown a micro-environment-sensitive system for covalent cross-linking of peptide-conjugated UCNP and triggering the accumulation of nanocrystals into the tumor site (Figure 9A).<sup>184</sup> This accumulation could effectively enhance the emission density of UCNP and intensify the production of reactive oxygen from the photosensitizers loaded on the nanocrystals for tumor treatment. In this work, targeted therapeutic evaluation was performed with UCNP platforms to investigate PDT besides in vivo photoacoustic imaging. As shown in Figure 9B, two groups of tumor-bearing mice

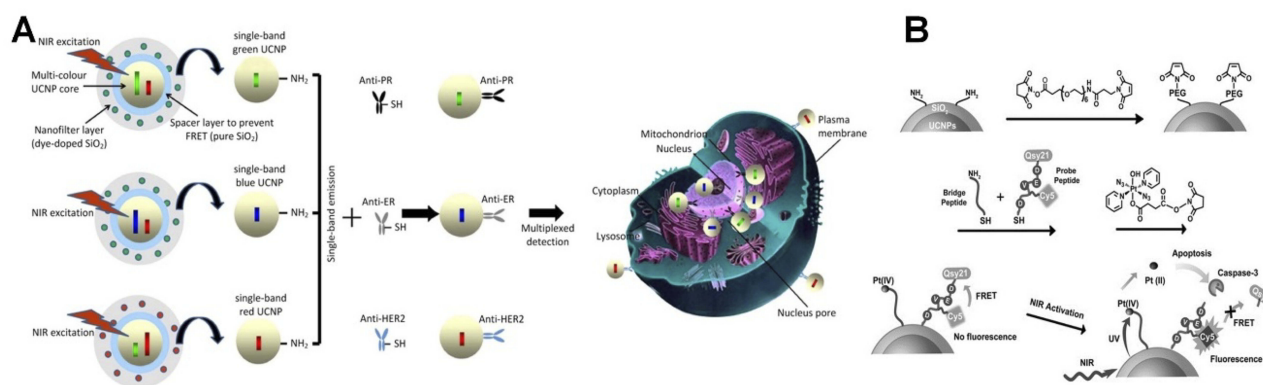


**Figure 8 (A)** Surface modified UCNP with organic dyes doped within silicon to get single emission from NPs. Antibody conjugation of these modified nanoparticles creates influential probes for multiplexed in situ molecular mapping of tumor biomarkers. Reproduced with permission from Zhou L, Wang R, Yao C, et al. Single-band upconversion nanoprobe for multiplexed simultaneous in situ molecular mapping of cancer biomarkers. *Nat Commun.* 2015;6:6938. <sup>172</sup> Copyright Springer Nature 2015. **(B)** Schematic representation of prodrug activation using NIR and intracellular apoptosis by UCL. Reproduced with permission from Min Y, Li J, Liu F, Yeow EKL, Xing B. Near-infrared light-mediated photoactivation of a platinum antitumor prodrug and simultaneous cellular apoptosis imaging by upconversion-luminescent nanoparticles. *Angew Chem Int Ed.* 2014;53(4):1012–1016. <sup>173</sup> Copyright 2013, John Wiley and Sons.

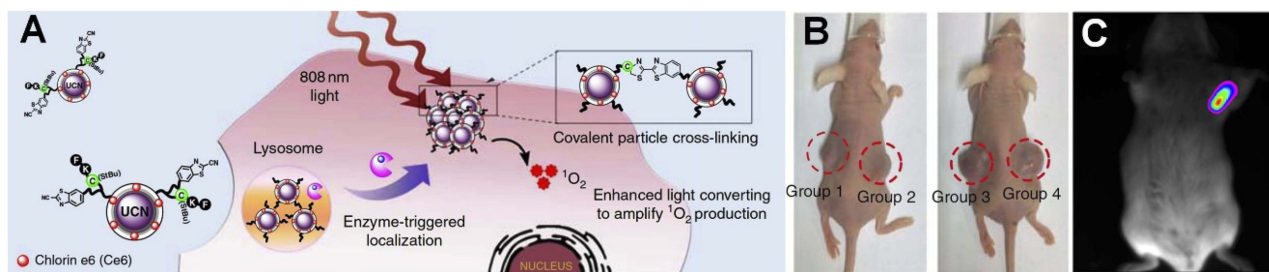


**Figure 9** (A) Schematic illustration of microenvironment-sensitive strategy. Triggering the accumulation of UCNP into the tumor. (B) Mice treated with PDT agent under NIR (G 1), control agent under NIR (G 2), PDT agent without NIR (G 3), and saline under NIR (G 4). Reproduced with permission from Ai X, Ho CJH, Aw J, et al. In vivo covalent cross-linking of photon-converted rare-earth nanostructures for tumour localization and theranostics. *Nat Commun.* 2016;7:10432. <sup>184</sup> (C) In vivo UCL imaging of a tumor-bearing mouse after intratumoral injection of UCNP solution into the tumor site. Reproduced with permission from Dai Y, Xiao H, Liu J, et al. In vivo multimodality imaging and cancer therapy by near-infrared light-triggered trans-platinum pro-drug-conjugated upconversion nanoparticles. *J Am Chem Soc.* 2013;135(50):18920–18929. <sup>185</sup> Copyright American Chemistry Society 2013.

underwent treatment. The results showed that the implanted tumor that was injected with PDT agent (group 1 [G 1]) could significantly inhibit the tumor growth under NIR irradiation in comparison with control agent under NIR (G 2), PDT agent without NIR (G 3), and tumor treated with NIR light alone (G 4).

Dai et al developed a type of nanotransducer with modification of core-shell  $Tm^{3+}$ -doped UCNP to trigger the platinum (iv) prodrug at the tumor site. <sup>185</sup> This photoactive platform, after entering the tumor cells via

endocytosis, could convert the deeply penetrating NIR light into UV and eradicate the tumor by on-site release of prodrug. Figure 9C shows the NIR to NIR UCL output observed from the tumor site after intratumoral injection of modified UCNP in the left axilla. An accurate multifunctional nanotheranostic agent was designed by Dai et al for sensitive diagnosis and in vivo treatment of tumors. <sup>186</sup> In this work, a complex of PDA-coated  $NaYF_4:Nd^{3+}/NaLuF_4$  nanocomposites was synthesized by core-shell strategy and employed for dual-modal imaging, namely NIR-II

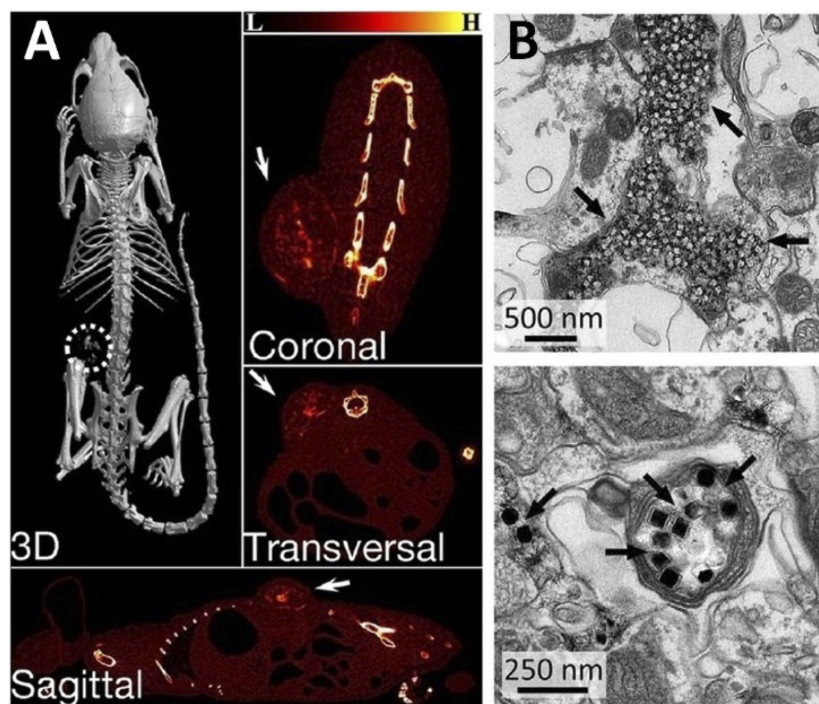


**Figure 10** (A) X-ray CT images of the tumor-bearing mice after intratumoral injection of NP/PDA suspension. Reproduced with permission from Dai Y, Yang D, Yu D, et al. Mussel-inspired polydopamine-coated lanthanide nanoparticles for NIR-II/CT dual imaging and photothermal therapy. *ACS Appl Mater Interfaces.* 2017;9(32):26674–26683. <sup>186</sup> Copyright American chemical society 2017. (B) Electron micrographs of UCNP distributed in the neuronal tissue. Black arrows indicate clusters of UCNP. Top image shows the distribution of most UCNP in extracellular space, and the bottom image shows the uptake of UCNP within an axon. From Chen S, Weitemier AZ, Zeng X, et al. Near-infrared deep brain stimulation via upconversion nanoparticle-mediated optogenetics. *Science.* 2018;359(6376):679. <sup>187</sup> Reprinted with permission from AAAS <https://science.sciencemag.org/content/359/6376/679>.

optical imaging and X-ray CT imaging, to acquire in vivo photothermal therapy (PTT) which might be a low-invasive therapy. The X-ray CT imaging, using these well-designed nanocomposites, could elucidate the important physiological and anatomical details of the implant tumor through excellent spatial resolution and depth for in vivo imaging. Furthermore, these particular nanocomposites are considered theoretically superior to the traditional iodine-based commercial X-ray imaging agent (Figure 10A). The substantive amine and hydroxyl groups on the surface of the NP@PDA nanocomposites could maintain the stability and dispersity of these nanocomposites in polar solvents for up to 2 months at ambient temperature.

### Applications in optogenetics studies

One of the most interesting recent applications with UCNPs is optogenetics studies in small animals, this is only feasible due to the deep penetration of NIR light into the body. A ground-breaking study by Chen et al showed the usage of molecularly tailored UCNPs in the presence of transcranial NIR light for deep brain stimulation in genetically-tagged neurons.<sup>187</sup> These UCNPs were precisely tuned to a particular wavelength by selective lanthanide ion doping. By incorporating  $Tm^{3+}$  into  $Yb^{3+}$ -doped host lattices, this produced blue emission matching the maximum absorption of channelrhodopsin-2 for activating neurons, while  $Yb^{3+}$ ,  $Er^{3+}$  couple was used to emit green light in a compatible way to activate halorhodopsin or archaerhodopsin for the purpose of inhibiting neuronal activity.

The concept of using UCNPs to mediate optogenetics is not new;<sup>188–192</sup> however, this study was the first to show minimally invasive deep brain stimulation in a mammalian system. This important demonstration overcomes the challenging issue of visible light being a limiting factor in optogenetics as used for manipulating neuronal activity in deep tissue penetration and remote therapy. The researchers were able to successfully evoke brain oscillations, through activation of inhibitory neurons in a specific area deep in the brain, and physiologically eliminate seizures by inhibiting excitatory cells in another specific region deep within the brain. After injecting an adeno-associated virus encoding an enhanced yellow fluorescent protein into the ventral tegmentum area (VTA) deep within the brain, they activated Cre-dependent gene expression of channelrhodopsin-2 in dopaminergic neurons for neuronal activation purposes. Four weeks following injection,

UCNPs were injected into the VTA region as well. Electron microscopy confirmed the presence of UCNPs primarily confined to the injection area with minimal dispersion, and that they were mainly distributed in extracellular spaces neighboring cell membranes and synaptic clefts, while a minority was shown as taken up by the neurons and clearly shown in their axons (Figure 10B). Real-time efficacy of the NIR-evoked excitation of these neurons was assessed by fast-scan cyclic voltammetry (FSCV) and confirmed dopamine release that was temporally confined to the transcranial NIR stimulation, with no dopamine release in control mice. With illumination at a distance of 0.5 mm, both the NIR and blue light triggered dopamine release in the ventral striatum area of the brain; and only NIR was able to elicit such a response in transcranial application. Besides neuronal activation, the researchers were also able to demonstrate the use of modified UCNPs for neuronal inhibition. It showed the ability of these modified UCNPs to inhibit activity of neurons in a different region of the brain, the hippocampus, which is primarily associated with memory formation and retention.

By demonstrating successful spectral tuning of UCNPs as compatible with the current toolbox of light-activated channels to the point of functionally activating and inhibiting neurons in various deep brain structures, these researchers have set a foundation for potential usage one day in human patients suffering from neurological conditions, such as Parkinson's disease, in which cumbersome electrical equipment must be implanted both in the brain and chest of patients and tuned manually in the clinic at regular intervals. Lin et al used a UCNPs-based miniature device for neural inhibition in mouse brain. In this study, a sealed package of  $NaYF_4:Yb,Er$  based UCNPs was placed precisely in animal brain for modulation of electrical activity of the neurons upon NIR (980 nm) irradiation.<sup>144</sup> This fiber-free technique allows the animal to move naturally and demonstrates the performance of deep brain inhibition with no attachments.

### Conclusion

In this review, we summarized the principle of physical/chemical properties and photoactivity behavior of UCNPs, including up-conversion mechanisms, crystals compositions, and efficient methods for synthesization, in order to convey a better understanding of their potential for further theranostic use. Following that, the strongest emphasis in this article was the conceptual application of these materials in medicine for a variety of purposes:

delivering, targeting, tumor therapy, and bioimaging in vitro and in vivo.

The discussions in this review article revealed that the unique functions of modified UCNPs in PDT by excitation of NIR light is a superior implement that might become a definite approach and inoffensive treatment for elimination of cancerous tissues. In addition to that, relatively high surface-area-to-volume ratio of these particles for loading the chemicals and biomaterials makes them an appropriate platform for drug and gene delivery for different diseases which need specific and selective targeting. Also, the high uptake of UCNPs by cells and tissues makes these functionalized fluorophore probes an indispensable tool for in vitro/in vivo imaging with high sensitivity and deep penetration of stimulators. In addition, reviewing general toxicity, the results from biodistribution in mouse body and excretion describe the reason for extending biomedical applications with these NPs.

Regarding the drawbacks of using UCNPs, it should be noted that due to unique optical properties and novelty of these materials in biochemistry and medicine, most of the commercial imaging equipment is not designed and compatible for direct application to UCNPs. Usually, the exciting light sources in confocal microscopes cover the range of UV and visible light, and the NIR sources of in vivo imaging machines are not focused and powerful enough to excite UCNPs; hence, scientists have to build their own homemade imaging instruments with suitable sources such as continuous wavelength lasers.

Overall, it is important to highlight the recently published reports, as they indicate how these novel NPs of different substances serve as appropriate alternatives to available mainstream techniques that otherwise pose arduous difficulties and limitations in detection and targeting, especially in hard-to-access areas of the body, such as deep brain structures. Harnessing the power of versatile UCNPs will be critical for developing modern and more tailored therapeutic approaches.

## Abbreviations

UCNPs, up-conversion nanoparticles; FDA, US Food and Drug Administration; NPs, nanoparticles; EPR, enhanced permeability and retention; QDs, quantum dots; PEG, polyethylene glycol; NIR, infrared; UV, ultraviolet; UCL, up-conversion luminescence; ESA, state absorption; ETU, up-conversion by energy transfer; TPA, two-photon absorption; CSU, cooperative sensitization up-conversion; CR, cross-relaxation; PA, photon avalanche; EMU, energy

migration-mediated up-conversion; QY, quantum yield; OM, oleylamine; OA, oleic acid; ODE, 1-octadecene; TEM, transmission electron microscopy; XRD, X-ray diffraction; EDTA, ethylene diamine tetra acetate; MRI, magnetic resonance imaging; CT, computed tomography; PET, positron emission tomography; FRET, fluorescence resonance energy transfer; GFP, green protein fluorescence; PDT, photodynamic therapy; CCPEB, cationic conjugated polyelectrolyte brush; PDA, polydopamine; ICG, indocyanine green; PTT, photothermal therapy; VTA, ventral tegmentum area; FSCV fast-scan cyclic voltammetry; Y, yttrium; Yb, ytterbium; Er, erbium; Tm, thulium; Gd, gadolinium.

## Acknowledgment

This project has received funding from the European Union's Horizon 2020 research and innovation programme under the Marie Skłodowska-Curie Grant Agreement No 701647.

## Disclosure

The authors declare no conflicts of interest in this work.

## References

1. Kim BYS, Rutka JT, Chan WCW. Nanomedicine. *N Engl J Med.* 2010;363(25):2434–2443. doi:10.1056/NEJMra0912273
2. Chow EK-H, Ho D. Cancer nanomedicine: from drug delivery to imaging. *Sci Transl Med.* 2013;5(216):216rv214–216rv214. doi:10.1126/scitranslmed.3005872
3. Kairdolf BA, Qian X, Nie S. Bioconjugated nanoparticles for biosensing, in vivo imaging, and medical diagnostics. *Anal Chem.* 2017;89(2):1015–1031. doi:10.1021/acs.analchem.6b04873
4. Liu Y, Miyoshi H, Nakamura M. Nanomedicine for drug delivery and imaging: a promising avenue for cancer therapy and diagnosis using targeted functional nanoparticles. *Int J Cancer.* 2007;120(12):2527–2537. doi:10.1002/ijc.22709
5. Shang L, Nienhaus K, Nienhaus GU. Engineered nanoparticles interacting with cells: size matters. *J Nanobiotechnology.* 2014;12:5. doi:10.1186/1477-3155-12-5
6. Popović Z, Liu W, Chauhan VP, et al. A nanoparticle size series for in vivo fluorescence imaging. *Angew Chem Int Ed.* 2010;49(46):8649–8652. doi:10.1002/anie.201003142
7. Khajeh M, Laurent S, Dastafkan K. Nanoabsorbents: classification, preparation, and applications (with emphasis on aqueous media). *Chem Rev.* 2013;113(10):7728–7768. doi:10.1021/cr400086v
8. Yamada T, Fukuhara K, Matsuoka K, et al. Nanoparticle chemisorption printing technique for conductive silver patterning with submicron resolution. *Nat Commun.* 2016;7:11402. doi:10.1038/ncomms11402
9. De Jong WH, Borm PJA. Drug delivery and nanoparticles: applications and hazards. *Int J Nanomedicine.* 2008;3(2):133–149.
10. Sun T, Zhang YS, Pang B, Hyun DC, Yang M, Xia Y. Engineered nanoparticles for drug delivery in cancer therapy. *Angew Chem Int Ed.* 2014;53(46):12320–12364. doi:10.1002/anie.201403036
11. De Crozals G, Bonnet R, Farre C, Chaix C. Nanoparticles with multiple properties for biomedical applications: a strategic guide. *Nano Today.* 2016;11(4):435–463. doi:10.1016/j.nantod.2016.07.002



12. Shen S, Wu Y, Liu Y, Wu D. High drug-loading nanomedicines: progress, current status, and prospects. *Int J Nanomedicine*. 2017;12:4085–4109. doi:10.2147/IJN.S132780
13. Wicki A, Witzigmann D, Balasubramanian V, Huwyler J. Nanomedicine in cancer therapy: challenges, opportunities, and clinical applications. *J Controlled Release*. 2015;200:138–157. doi:10.1016/j.jconrel.2014.12.030
14. Prencipe G, Tabakman SM, Welsher K, et al. PEG branched polymer for functionalization of nanomaterials with ultralong blood circulation. *J Am Chem Soc*. 2009;131(13):4783–4787. doi:10.1021/ja809086q
15. Bobo D, Robinson KJ, Islam J, Thurecht KJ, Corrie SR. Nanoparticle-based medicines: a review of FDA-approved materials and clinical trials to date. *Pharm Res*. 2016;33(10):2373–2387. doi:10.1007/s11095-016-1958-5
16. Ventola CL. Progress in nanomedicine: approved and investigational nanodrugs. *PT*. 2017;42(12):742–755.
17. Singh R, Lillard JW. Nanoparticle-based targeted drug delivery. *Exp Mol Pathol*. 2009;86(3):215–223. doi:10.1016/j.yexmp.2008.12.004
18. Barreto JA, O'Malley W, Kubeil M, Graham B, Stephan H, Spiccia L. Nanomaterials: applications in cancer imaging and therapy. *Adv Mater*. 2011;23(12):H18–H40. doi:10.1002/adma.201100140
19. Rwei AY, Wang W, Kohane DS. Photoresponsive nanoparticles for drug delivery. *Nano Today*. 2015;10(4):451–467. doi:10.1016/j.nantod.2015.06.004
20. Kou L, Sun J, Zhai Y, He Z. The endocytosis and intracellular fate of nanomedicines: implication for rational design. *Asian J Pharm Sci*. 2013;8(1):1–10. doi:10.1016/j.ajps.2013.07.001
21. Yameen B, Choi WI, Vilos C, Swami A, Shi J, Farokhzad OC. Insight into nanoparticle cellular uptake and intracellular targeting. *J Controlled Release*. 2014;190:485–499. doi:10.1016/j.jconrel.2014.06.038
22. Min Y, Roche KC, Tian S, et al. Antigen-capturing nanoparticles improve the abscopal effect and cancer immunotherapy. *Nat Nano*. 2017. advance online publication. doi:10.1038/nnano.2017.113
23. Singh L, Kruger HG, Maguire GEM, Govender T, Parboosing R. The role of nanotechnology in the treatment of viral infections. *Ther Adv Infect Dis*. 2017;4(4):105–131. doi:10.1177/2049936117713593
24. Gendelman HE, Anantharam V, Bronich T, et al. Nanoneurotherapeutics for degenerative, inflammatory, and infectious nervous system diseases. *Nanomed. Nanotechnol Biol Med*. 2015;11(3):751–767. doi:10.1016/j.nano.2014.12.014
25. Park S-M, Aalipour A, Vermesh O, Yu JH, Gambhir SS. Towards clinically translatable in vivo nanodiagnoses. *Nat Rev Mater*. 2017;2:17014. doi:10.1038/natrevmats.2017.14
26. Jennifer M, Maciej W. Nanoparticle technology as a double-edged sword: cytotoxic, genotoxic and epigenetic effects on living cells. *J Biomater Nanobiotechnol*. 2013;04(01):11. doi:10.4236/jbnb.2013.41008
27. Choueiri RM, Galati E, Thérien-Aubin H, et al. Surface patterning of nanoparticles with polymer patches. *Nature*. 2016;538(7623):79–83. doi:10.1038/nature19089
28. Zhang L, Li Y, Yu JC. Chemical modification of inorganic nanostructures for targeted and controlled drug delivery in cancer treatment. *J Mater Chem B*. 2014;2(5):452–470. doi:10.1039/C3TB21196G
29. Shen J, Zhao L, Han G. Lanthanide-doped upconverting luminescent nanoparticle platforms for optical imaging-guided drug delivery and therapy. *Adv Drug Deliv Rev*. 2013;65(5):744–755. doi:10.1016/j.addr.2012.05.007
30. Davis ME, Chen Z, Shin DM. Nanoparticle therapeutics: an emerging treatment modality for cancer. *Nat Rev Drug Discov*. 2008;7(9):771–782. doi:10.1038/nrd2614
31. Cao Y, Jin R, Mirkin CA. DNA-modified core-shell Ag/Au nanoparticles. *J Am Chem Soc*. 2001;123(32):7961–7962. doi:10.1021/ja011342n
32. Feng X, Yao J, Gao X, et al. Multi-targeting peptide-functionalized nanoparticles recognized vasculogenic mimicry, tumor neovasculature, and glioma cells for enhanced anti-glioma therapy. *ACS Appl Mater Interfaces*. 2015;7(50):27885–27899. doi:10.1021/acsami.5b09934
33. Lu J, Shi M, Shoichet MS. Click chemistry functionalized polymeric nanoparticles target corneal epithelial cells through RGD-cell surface receptors. *Bioconjug Chem*. 2009;20(1):87–94. doi:10.1021/bc8003167
34. Sapsford KE, Algar WR, Berti L, et al. Functionalizing nanoparticles with biological molecules: developing chemistries that facilitate nanotechnology. *Chem Rev*. 2013;113(3):1904–2074. doi:10.1021/cr300143v
35. Banerjee SS, Aher N, Patil R, Khandare J. Poly(ethylene glycol)-prodrug conjugates: concept, design, and applications. *J Drug Deliv*. 2012;2012:103973. doi:10.1155/2012/103973
36. Tao Z, Hong G, Shinji C, et al. Biological imaging using nanoparticles of small organic molecules with fluorescence emission at wavelengths longer than 1000 nm. *Angew Chem*. 2013;125(49):13240–13244. doi:10.1002/ange.201307346
37. Song J, Huang P, Chen X. Preparation of plasmonic vesicles from amphiphilic gold nanocrystals grafted with polymer brushes. *Nat Protoc*. 2016;11:2287. doi:10.1038/nprot.2016.137
38. Cheng L, Song J, Yin J, Duan H. Self-assembled plasmonic dimers of amphiphilic gold nanocrystals. *J Phys Chem Lett*. 2011;2(17):2258–2262. doi:10.1021/jz201011b
39. Liu Y, Lu Y, Yang X, et al. Amplified stimulated emission in upconversion nanoparticles for super-resolution nanoscopy. *Nature*. 2017;543:229. doi:10.1038/nature21366
40. Wang M, Zhu Y, Mao C. Synthesis of NIR-responsive NaYF<sub>4</sub>: Yb, Er/Upconversion fluorescent nanoparticles using an optimized solvothermal method and their applications in enhanced development of latent fingerprints on various smooth substrates. *Langmuir*. 2015;31(25):7084–7090. doi:10.1021/acs.langmuir.5b01151
41. Zhou B, Shi B, Jin D, Liu X. Controlling upconversion nanocrystals for emerging applications. *Nat Nanotechnol*. 2015;10:924. doi:10.1038/nnano.2015.251
42. Zhu H, Chen X, Jin LM, Wang QJ, Wang F, Yu SF. Amplified spontaneous emission and lasing from lanthanide-doped up-conversion nanocrystals. *ACS Nano*. 2013;7(12):11420–11426. doi:10.1021/nn405387t
43. Yao W, Tian Q, Wu W. Tunable emissions of upconversion fluorescence for security applications. *Adv Opt Mater*. 2019;7(6):1801171. doi:10.1002/adom.v7.6
44. Wang J, Wei T, Li X, et al. Near-infrared-light-mediated imaging of latent fingerprints based on molecular recognition. *Angew Chem Int Ed*. 2014;53(6):1616–1620. doi:10.1002/anie.201308843
45. Zhang C, Zhou H-P, Liao L-Y, et al. Luminescence modulation of ordered upconversion nanopatterns by a photochromic diarylethene: rewritable optical storage with nondestructive readout. *Adv Mater*. 2010;22(5):633–637. doi:10.1002/adma.200901722
46. Liu H, Xu J, Wang H, et al. Tunable Resonator-Upconverted Emission (TRUE) color printing and applications in optical security. *Adv Mater*. 2019;31(15):1807900. doi:10.1002/adma.201802348
47. Meruga JM, Baride A, Cross W, Kellar JJ, May PS. Red-green-blue printing using luminescence-upconversion inks. *J Mater Chem C*. 2014;2(12):2221–2227. doi:10.1039/c3tc32233e
48. You M, Zhong J, Hong Y, Duan Z, Lin M, Xu F. Inkjet printing of upconversion nanoparticles for anti-counterfeit applications. *Nanoscale*. 2015;7(10):4423–4431. doi:10.1039/c4nr06944g

49. You M, Lin M, Wang S, et al. Three-dimensional quick response code based on inkjet printing of upconversion fluorescent nanoparticles for drug anti-counterfeiting. *Nanoscale*. 2016;8(19):10096–10104. doi:10.1039/c6nr01353h
50. Bloembergen N. Solid state infrared quantum counters. *Phys Rev Lett*. 1959;2(3):84–85. doi:10.1103/PhysRevLett.2.84
51. Auzel F. Compteur Quantique Par Transfert Denergie Entre Deux Ions De Terres Rares Dans Un Tungstate Mixte Et Dans Un Verre. *CR Acad Sci Paris*. 1966;262:1016–1019.
52. Dodson CM, Zia R. Magnetic dipole and electric quadrupole transitions in the trivalent lanthanide series: calculated emission rates and oscillator strengths. *Phys Rev B*. 2012;86(12):125102. doi:10.1103/PhysRevB.86.125102
53. Dong H, Sun L-D, Yan C-H. Energy transfer in lanthanide upconversion studies for extended optical applications. *Chem Soc Rev*. 2015;44(6):1608–1634. doi:10.1039/c4cs00188e
54. Seth M, Dolg M, Fulde P, Schwerdtfeger P. Lanthanide and actinide contractions: relativistic and shell structure effects. *J Am Chem Soc*. 1995;117(24):6597–6598. doi:10.1021/ja00129a026
55. Li X, Zhang F, Zhao D. Highly efficient lanthanide upconverting nanomaterials: progresses and challenges. *Nano Today*. 2013;8(6):643–676. doi:10.1016/j.nantod.2013.11.003
56. Li X, Zhang F, Zhao D. Lab on upconversion nanoparticles: optical properties and applications engineering via designed nanostructure. *Chem Soc Rev*. 2015;44(6):1346–1378. doi:10.1039/c4cs00163j
57. Nakazawa E, Shionoya S. Energy transfer between trivalent rare-earth ions in inorganic solids. *J Chem Phys*. 1967;47(9):3211–3219. doi:10.1063/1.1712377
58. Balestrieri M, Colis S, Gallart M, et al. Photoluminescence properties of rare earth (Nd, Yb, Sm, Pr)-doped CeO<sub>2</sub> pellets prepared by solid-state reaction. *J Mater Chem C*. 2015;3(27):7014–7021. doi:10.1039/C5TC00075K
59. Downing E, Hesselink L, Ralston J, Macfarlane R. A three-color, solid-state, three-dimensional display. *Science*. 1996;273(5279):1185–1189. doi:10.1126/science.273.5279.1185
60. Sivakumar S, van Veggel FCJM, Raudsepp M. Bright white light through up-conversion of a single NIR source from Sol–Gel-derived thin film made with Ln<sup>3+</sup>-Doped LaF<sub>3</sub> nanoparticles. *J Am Chem Soc*. 2005;127(36):12464–12465. doi:10.1021/ja052583o
61. Sun L-D, Dong H, Zhang P-Z, Yan C-H. Upconversion of rare earth nanomaterials. *Annu Rev Phys Chem*. 2015;66(1):619–642. doi:10.1146/annurev-physchem-040214-121344
62. Wang F, Deng R, Wang J, et al. Tuning upconversion through energy migration in core–shell nanoparticles. *Nat Mater*. 2011;10:968. doi:10.1038/nmat3084
63. Wang F, Liu X. Recent advances in the chemistry of lanthanide-doped upconversion nanocrystals. *Chem Soc Rev*. 2009;38(4):976–989. doi:10.1039/b809132n
64. Ning K, Chao-Chao A, Ya-Ming Z, Zuo W, Lei R. Facile synthesis of upconversion nanoparticles with high purity using lanthanide oleate compounds. *Nanotechnology*. 2018;29(7):075601. doi:10.1088/1361-6528/aa96ee
65. Liu G. Advances in the theoretical understanding of photon upconversion in rare-earth activated nanophosphors. *Chem Soc Rev*. 2015;44(6):1635–1652. doi:10.1039/c4cs00187g
66. Suyver JF, Grimm J, van Veen MK, Biner D, Krämer KW, Güdel HU. Upconversion spectroscopy and properties of NaYF<sub>4</sub> doped with Er<sup>3+</sup>, Tm<sup>3+</sup> and/or Yb<sup>3+</sup>. *J Lumin*. 2006;117(1):1–12. doi:10.1016/j.jlumin.2005.03.011
67. Wang F, Deng R, Wang J, et al. Tuning upconversion through energy migration in core–shell nanoparticles. *Nat Mater*. 2011;10(12):968–973. doi:10.1038/nmat3149
68. Chen G, Qiu H, Prasad PN, Chen X. Upconversion nanoparticles: design, nanochemistry, and applications in theranostics. *Chem Rev*. 2014;114(10):5161–5214. doi:10.1021/cr400425h
69. Gai S, Li C, Yang P, Lin J. Recent progress in rare earth micro/nanocrystals: soft chemical synthesis, luminescent properties, and biomedical applications. *Chem Rev*. 2014;114(4):2343–2389. doi:10.1021/cr4001594
70. Yang D, Dai Y, Liu J, et al. Ultra-small BaGdF<sub>5</sub>-based upconversion nanoparticles as drug carriers and multimodal imaging probes. *Biomaterials*. 2014;35(6):2011–2023. doi:10.1016/j.biomaterials.2013.11.018
71. Xu D, Li A, Yao L, Lin H, Yang S, Zhang Y. Lanthanide-doped KLu<sub>2</sub>F<sub>7</sub> nanoparticles with high upconversion luminescence performance: a comparative study by judd-ofelt analysis and energy transfer mechanistic investigation. *Sci Rep*. 2017;7:43189. doi:10.1038/srep43189
72. Liu D, Xu X, Du Y, et al. Three-dimensional controlled growth of monodisperse sub-50 nm heterogeneous nanocrystals. *Nat Commun*. 2016;7:10254. doi:10.1038/ncomms10254
73. Gargas DJ, Chan EM, Ostrowski AD, et al. Engineering bright sub-10-nm upconverting nanocrystals for single-molecule imaging. *Nat Nanotechnol*. 2014;9:300. doi:10.1038/nnano.2014.29
74. Wang F, Han Y, Lim CS, et al. Simultaneous phase and size control of upconversion nanocrystals through lanthanide doping. *Nature*. 2010;463(7284):1061–1065. doi:10.1038/nature08777
75. Gu M, Zhang Q, Lamon S. Nanomaterials for optical data storage. *Nat Rev Mater*. 2016;1:16070. doi:10.1038/natrevmats.2016.70
76. Zhou B, Shi B, Jin D, Liu X. Controlling upconversion nanocrystals for emerging applications. *Nat Nano*. 2015;10(11):924–936. doi:10.1038/nnano.2015.251
77. Wen S, Zhou J, Zheng K, Bednarkiewicz A, Liu X, Jin D. Advances in highly doped upconversion nanoparticles. *Nat Commun*. 2018;9(1):2415. doi:10.1038/s41467-018-04813-5
78. Zhao J, Jin D, Schartner EP, et al. Single-nanocrystal sensitivity achieved by enhanced upconversion luminescence. *Nat Nanotechnol*. 2013;8:729. doi:10.1038/nnano.2013.171
79. Dexter DL, Schulman JH. Theory of concentration quenching in inorganic phosphors. *J Chem Phys*. 1954;22(6):1063–1070. doi:10.1063/1.1740265
80. Tu L, Liu X, Wu F, Zhang H. Excitation energy migration dynamics in upconversion nanomaterials. *Chem Soc Rev*. 2015;44(6):1331–1345. doi:10.1039/c4cs00168k
81. Li M, Hao ZH, Peng XN, Li JB, Yu XF, Wang QQ. Controllable energy transfer in fluorescence upconversion of NdF<sub>3</sub> and NaNdF<sub>4</sub> nanocrystals. *Opt Express*. 2010;18(4):3364–3369. doi:10.1364/OE.18.003364
82. Taniguchi T, Murakami T, Funatsu A, Hatakeyama K, Koinuma M, Matsumoto Y. Reversibly tunable upconversion luminescence by host–guest chemistry. *Inorg Chem*. 2014;53(17):9151–9155. doi:10.1021/ic501129y
83. Deng R, Xie X, Vendrell M, Chang Y-T, Liu X. Intracellular glutathione detection using mno<sub>2</sub>-nanosheet-modified upconversion nanoparticles. *J Am Chem Soc*. 2011;133(50):20168–20171. doi:10.1021/ja2100774
84. Ran W, Wang L, Tan L, Qu D, Shi J. Remote control effect of Li<sup>+</sup>, Na<sup>+</sup>, K<sup>+</sup> ions on the super energy transfer process in ZnMoO<sub>4</sub>: Eu<sup>3+</sup>, Bi<sup>3+</sup> phosphors. *Sci Rep*. 2016;6:27657. doi:10.1038/srep27657
85. Zhong Y, Rostami I, Wang Z, Dai H, Hu Z. Energy migration engineering of bright rare-earth upconversion nanoparticles for excitation by light-emitting diodes. *Adv Mater*. 2015;27(41):6418–6422. doi:10.1002/adma.201502272
86. Zhong Y, Tian G, Gu Z, et al. Elimination of photon quenching by a transition layer to fabricate a quenching-shield sandwich structure for 800 nm excited upconversion luminescence of Nd<sup>3+</sup>-sensitized nanoparticles. *Adv Mater*. 2014;26(18):2831–2837. doi:10.1002/adma.201304903

87. Wang F, Deng R, Liu X. Preparation of core-shell NaGdF<sub>4</sub> nanoparticles doped with luminescent lanthanide ions to be used as upconversion-based probes. *Nat Protoc.* 2014;9:1634. doi:10.1038/nprot.2014.111
88. Chen X, Peng D, Ju Q, Wang F. Photon upconversion in core-shell nanoparticles. *Chem Soc Rev.* 2015;44(6):1318–1330. doi:10.1039/c4cs00151f
89. Wang F, Deng R, Liu X. Preparation of core-shell NaGdF<sub>4</sub> nanoparticles doped with luminescent lanthanide ions to be used as upconversion-based probes. *Nat Protoc.* 2014;9(7):1634–1644. doi:10.1038/nprot.2014.111
90. Li X, Shen D, Yang J, et al. Successive layer-by-layer strategy for multi-shell epitaxial growth: shell thickness and doping position dependence in upconverting optical properties. *Chem Mater.* 2013;25(1):106–112. doi:10.1021/cm3033498
91. Chen G, Roy I, Yang C, et al. Nanochemistry and nanomedicine for nanoparticle-based diagnostics and therapy. *Chem Rev.* 2016;116(5):2826–2885. doi:10.1021/acs.chemrev.5b00148
92. Huang P, Tu D, Zheng W, Zhou S, Chen Z, Chen X. Inorganic lanthanide nanoprobe for background-free luminescent bioassays. *Sci China Mater.* 2015;58(2):156–177. doi:10.1007/s40843-015-0019-4
93. Mir SH, Nagahara LA, Thundat T, Mokarian-Tabari P, Furukawa H, Khosla A. Review—organic-inorganic hybrid functional materials: an integrated platform for applied technologies. *J Electrochem Soc.* 2018;165(8):B3137–B3156. doi:10.1149/2.0191808jes
94. Kuhn S, Tiegel M, Herrmann A, et al. Effect of hydroxyl concentration on Yb<sup>3+</sup> luminescence properties in a peraluminous lithium-alumino-silicate glass. *Opt Mater Express.* 2015;5(2):430–440. doi:10.1364/OME.5.000430
95. Yan Y, Faber AJ, de Waal H. Luminescence quenching by OH groups in highly Er-doped phosphate glasses. *J Non Cryst Solids.* 1995;181(3):283–290. doi:10.1016/S0022-3093(94)00528-1
96. Su Q, Han S, Xie X, et al. The effect of surface coating on energy migration-mediated upconversion. *J Am Chem Soc.* 2012;134(51):20849–20857. doi:10.1021/ja3111048
97. Yi G-S, Chow G-M. Water-soluble NaYF<sub>4</sub>: Yb,Er(Tm)/NaYF<sub>4</sub>/polymercore/shell/shell nanoparticles with significant enhancement of upconversion fluorescence. *Chem Mater.* 2007;19(3):341–343. doi:10.1021/cm062447y
98. Zhang F, Che R, Li X, et al. Direct imaging the upconversion nanocrystal core/shell structure at the subnanometer level: shell thickness dependence in upconverting optical properties. *Nano Lett.* 2012;12(6):2852–2858. doi:10.1021/nl300421n
99. Zhan Q, He S, Qian J, Cheng H, Cai F. Optimization of optical excitation of upconversion nanoparticles for rapid microscopy and deeper tissue imaging with higher quantum yield. *Theranostics.* 2013;3(5):306–316. doi:10.7150/thno.6007
100. Wisser MD, Fischer S, Siefe C, Alivisatos AP, Salleo A, Dionne JA. Improving quantum yield of upconverting nanoparticles in aqueous media via emission sensitization. *Nano Lett.* 2018;18(4):2689–2695. doi:10.1021/acs.nanolett.8b00634
101. Rafik N, Qing Y, CJ A. The fluoride host: nucleation, growth, and upconversion of lanthanide-doped nanoparticles. *Adv Opt Mater.* 2015;3(4):482–509. doi:10.1002/adom.201400628
102. Mi C, Tian Z, Cao C, Wang Z, Mao C, Xu S. Novel microwave-assisted solvothermal synthesis of NaYF<sub>4</sub>: Yb,ErUpconversion nanoparticles and their application in cancer cell imaging. *Langmuir.* 2011;27(23):14632–14637. doi:10.1021/la204015m
103. Murali G, Lee BH, Mishra RK, et al. Synthesis, luminescence properties, and growth mechanisms of YF<sub>3</sub>: Yb<sup>3+</sup>/Er<sup>3+</sup>nanoplates. *J Mater Chem C.* 2015;3(39):10107–10113. doi:10.1039/C5TC02034D
104. Liu X, Zhang X, Tian G, et al. A simple and efficient synthetic route for preparation of NaYF<sub>4</sub> upconversion nanoparticles by thermo-decomposition of rare-earth oleates. *CrystEngComm.* 2014;16(25):5650–5661. doi:10.1021/acs.chemrev.5b00148
105. Zhong Y, Ma Z, Zhu S, et al. Boosting the down-shifting luminescence of rare-earth nanocrystals for biological imaging beyond 1500 nm. *Nat Commun.* 2017;8(1):737. doi:10.1038/s41467-017-00917-6
106. Mai H-X, Zhang Y-W, Sun L-D, Yan C-H. Size- and phase-controlled synthesis of monodisperse NaYF<sub>4</sub>: Yb,ErNanocrystals from a unique delayed nucleation pathway monitored with upconversion spectroscopy. *J Phys Chem C.* 2007;111(37):13730–13739. doi:10.1021/jp073919e
107. Mai H-X, Zhang Y-W, Si R, et al. High-quality sodium rare-earth fluoride nanocrystals: controlled synthesis and optical properties. *J Am Chem Soc.* 2006;128(19):6426–6436. doi:10.1021/ja060212h
108. Chen J, Zhao JX. Upconversion nanomaterials: synthesis, mechanism, and applications in sensing. *Sensors.* 2012;12(3):2414. doi:10.3390/s120302414
109. Chen G, Shen J, Ohulchanskyy TY, et al. (α-NaYbF<sub>4</sub>:Tm<sup>3+</sup>)/CaF<sub>2</sub>Core/shell nanoparticles with efficient near-infrared to near-infrared upconversion for high-contrast deep tissue bioimaging. *ACS Nano.* 2012;6(9):8280–8287. doi:10.1021/nn302972r
110. Dunne PW, Munn AS, Starkey CL, Huddle TA, Lester EH. Continuous-flow hydrothermal synthesis for the production of inorganic nanomaterials. *Philos Trans R Soc Lond A.* 2015;373(2057):20150015. doi:10.1098/rsta.2015.0015
111. Ma Y, Chen M, Li M. Hydrothermal synthesis of hydrophilic NaYF<sub>4</sub>: Yb,Ernanoparticles with bright upconversion luminescence as biological label. *Mater Lett.* 2015;139:22–25. doi:10.1016/j.matlet.2014.10.042
112. Li C, Quan Z, Yang J, Yang P, Lin J. Highly uniform and monodisperse β-NaYF<sub>4</sub>: Ln<sup>3+</sup>(Ln = Eu, Tb, Yb/ Er, and Yb/Tm) hexagonal microprism crystals: hydrothermal synthesis and luminescent properties. *Inorg Chem.* 2007;46(16):6329–6337. doi:10.1021/ic070335i
113. Zeng JH, Su J, Li ZH, Yan RX, Li YD. Synthesis and upconversion luminescence of hexagonal-phase NaYF<sub>4</sub>: Yb,Er<sup>3+</sup> phosphors of controlled size and morphology. *Adv Mater.* 2005;17(17):2119–2123. doi:10.1002/adma.200402046
114. Zhou R, Li X. Effect of EDTA on the formation and upconversion of NaYF<sub>4</sub>:Yb<sup>3+</sup>/Er<sup>3+</sup>. *Opt Mater Express.* 2016;6(4):1313–1320. doi:10.1364/OME.6.001313
115. Wang Y, Cai R, Liu Z. Controlled synthesis of NaYF<sub>4</sub>: Yb, Er nanocrystals with upconversion fluorescence via a facile hydrothermal procedure in aqueous solution. *CrystEngComm.* 2011;13(6):1772–1774. doi:10.1039/c0ce00708k
116. Menyuk N, Dwight K, Pierce JW. NaYF<sub>4</sub>: Yb,Er—an efficient upconversion phosphor. *Appl Phys Lett.* 1972;21(4):159–161. doi:10.1063/1.1654325
117. Shen H, Wang F, Fan X, Wang M. Synthesis of LaF<sub>3</sub>: Yb<sup>3+</sup>,Ln<sup>3+</sup> nanoparticles with improved upconversion luminescence. *J Exp Nanosci.* 2007;2(4):303–311. doi:10.1080/17458080701724943
118. Zhang F, Wan Y, Yu T, et al. Uniform nanostructured arrays of sodium rare-earth fluorides for highly efficient multicolor upconversion luminescence. *Angew Chem.* 2007;119(42):8122–8125. doi:10.1002/ange.200702519
119. Qiu P, Zhou N, Chen H, Zhang C, Gao G, Cui D. Recent advances in lanthanide-doped upconversion nanomaterials: synthesis, nanostructures and surface modification. *Nanoscale.* 2013;5(23):11512–11525. doi:10.1039/c3nr03642a
120. Ye X, Collins JE, Kang Y, et al. Morphologically controlled synthesis of colloidal upconversion nanophosphors and their shape-directed self-assembly. *Proc Natl Acad Sci.* 2010;107(52):22430–22435. doi:10.1073/pnas.1008958107
121. Dong C, van Veggel FCJM. Cation exchange in lanthanide fluoride nanoparticles. *ACS Nano.* 2009;3(1):123–130. doi:10.1021/nn8004747

122. Shao B, Zhao Q, Jia Y, et al. A novel synthetic route towards monodisperse  $\beta$ -NaYF<sub>4</sub>: Ln<sup>3+</sup>/micro/nanocrystals from layered rare-earth hydroxides at ultra low temperature. *Chem Commun.* 2014;50(84):12706–12709. doi:10.1039/c4cc05191b
123. Lei P, An R, Yao S, et al. Ultrafast synthesis of novel hexagonal phase NaBiF<sub>4</sub> upconversion nanoparticles at room temperature. *Adv Mater.* 2017;29:22. doi:10.1002/adma.201700681
124. Feldmann C, Jungk H-O. Preparation of sub-micrometer LnPO<sub>4</sub> particles (Ln = La, Ce). *J Mater Sci.* 2002;37(15):3251–3254. doi:10.1023/A:1016131016637
125. Feldmann C, Jungk H-O. Polyol-mediated preparation of nanoscale oxide particles. *Angew Chem Int Ed.* 2001;40(2):359–362. doi:10.1002/(ISSN)1521-3773
126. Chen J, Herricks T, Xia Y. Polyol synthesis of platinum nanostructures: control of morphology through the manipulation of reduction kinetics. *Angew Chem Int Ed.* 2005;44(17):2589–2592. doi:10.1002/anie.200462668
127. Dong H, Du S-R, Zheng X-Y, et al. Lanthanide nanoparticles: from design toward bioimaging and therapy. *Chem Rev.* 2015;115(19):10725–10815. doi:10.1021/acs.chemrev.5b00091
128. Gnach A, Lipinski T, Bednarkiewicz A, Rybka J, Capobianco JA. Upconverting nanoparticles: assessing the toxicity. *Chem Soc Rev.* 2015;44(6):1561–1584. doi:10.1039/c4cs00177j
129. Xiong L, Yang T, Yang Y, Xu C, Li F. Long-term in vivo biodistribution imaging and toxicity of polyacrylic acid-coated upconversion nanophosphors. *Biomaterials.* 2010;31(27):7078–7085. doi:10.1016/j.biomaterials.2010.05.065
130. Wang M, Abbineni G, Clevenger A, Mao C, Xu S. Upconversion nanoparticles: synthesis, surface modification and biological applications. *Nanomed. Nanotechnol Biol Med.* 2011;7(6):710–729. doi:10.1016/j.nano.2011.02.013
131. He S, Krippes K, Ritz S, et al. Ultralow-intensity near-infrared light induces drug delivery by upconverting nanoparticles. *Chem Commun.* 2015;51(2):431–434. doi:10.1039/c4cc07489k
132. Li N, Wen X, Liu J, Wang B, Zhan Q, He S. Yb<sup>3+</sup>-enhanced UCNP@SiO<sub>2</sub> nanocomposites for consecutive imaging, photothermal-controlled drug delivery and cancer therapy. *Opt Mater Express.* 2016;6(4):1161–1171. doi:10.1364/OME.6.001161
133. Das GK, Stark DT, Kennedy IM. Potential toxicity of up-converting nanoparticles encapsulated with a bilayer formed by ligand attraction. *Langmuir.* 2014;30(27):8167–8176. doi:10.1021/la501595f
134. Wong PT, Chen D, Tang S, et al. Modular integration of upconverting nanocrystal–dendrimer composites for folate receptor-specific NIR imaging and light-triggered drug release. *Small.* 2015;11(45):6078–6090. doi:10.1002/sml.201501575
135. Wysokińska E, Cichos J, Kowalczyk A, et al. Toxicity mechanism of low doses of NaGdF<sub>4</sub>: Yb(3+),Er(3+)upconverting nanoparticles in activated macrophage cell lines. *Biomolecules.* 2019;9(1):14. doi:10.3390/biom9060228
136. Guller AE, Generalova AN, Petersen EV, et al. Cytotoxicity and non-specific cellular uptake of bare and surface-modified upconversion nanoparticles in human skin cells. *Nano Res.* 2015;8(5):1546–1562. doi:10.1007/s12274-014-0641-6
137. Wysokińska E, Cichos J, Ziolo E, et al. Cytotoxic interactions of bare and coated NaGdF<sub>4</sub>: Yb<sup>3+</sup>:Er<sup>3+</sup>nanoparticles with macrophage and fibroblast cells. *Toxicol in Vitro.* 2016;32:16–25. doi:10.1016/j.tiv.2015.11.021
138. Ramasamy P, Chandra P, Rhee SW, Kim J. Enhanced upconversion luminescence in NaGdF<sub>4</sub>: Yb,Ernanocrystals by Fe<sup>3+</sup> doping and their application in bioimaging. *Nanoscale.* 2013;5(18):8711–8717. doi:10.1039/c3nr01608k
139. Pem B, González-Mancebo D, Moros M, et al. Biocompatibility assessment of up-and down-converting nanoparticles: implications of interferences with in vitro assays. *Method Appl Fluoresc.* 2018;7(1):014001. doi:10.1088/2050-6120/aae9c8
140. González-Béjar M, Francés-Soriano L, Pérez-Prieto J. Upconversion nanoparticles for bioimaging and regenerative medicine. *Front Bioeng Biotechnol.* 2016;4:47. doi:10.3389/fbioe.2016.00047
141. Wang F, Banerjee D, Liu Y, Chen X, Liu X. Upconversion nanoparticles in biological labeling, imaging, and therapy. *Analyt.* 2010;135(8):1839–1854. doi:10.1039/c0an00144a
142. Chatterjee DK, Rufaihah AJ, Zhang Y. Upconversion fluorescence imaging of cells and small animals using lanthanide doped nanocrystals. *Biomaterials.* 2008;29(7):937–943. doi:10.1016/j.biomaterials.2007.10.051
143. Park YI, Lee KT, Suh YD, Hyeon T. Upconverting nanoparticles: a versatile platform for wide-field two-photon microscopy and multimodal in vivo imaging. *Chem Soc Rev.* 2015;44(6):1302–1317. doi:10.1039/c4cs00173g
144. Lin X, Chen X, Zhang W, et al. Core-shell-shell upconversion nanoparticles with enhanced emission for wireless optogenetic inhibition. *Nano Lett.* 2018;18(2):948–956. doi:10.1021/acs.nanolett.7b04339
145. Tsang M-K, Bai G, Hao J. Stimuli responsive upconversion luminescence nanomaterials and films for various applications. *Chem Soc Rev.* 2015;44(6):1585–1607. doi:10.1039/c4cs00171k
146. Xu CT, Zhan Q, Liu H, et al. Upconverting nanoparticles for pre-clinical diffuse optical imaging, microscopy and sensing: current trends and future challenges. *Laser Photon Rev.* 2013;7(5):663–697. doi:10.1002/lpor.201200052
147. Li X, Yi Z, Xue Z, Zeng S, Liu H. Multifunctional BaYbF<sub>5</sub>: Gd/Er upconversion nanoparticles for in vivo tri-modal upconversion optical, X-ray computed tomography and magnetic resonance imaging. *Mater Sci Eng.* 2017;75:510–516. doi:10.1016/j.msec.2017.02.085
148. Guan M, Dong H, Ge J, et al. Multifunctional upconversion-nanoparticles-trimethylpyridylporphyrin-fullerene nanocomposite: a near-infrared light-triggered theranostic platform for imaging-guided photodynamic therapy. *NPG Asia Mater.* 2015;7:e205. doi:10.1038/am.2015.82
149. Zhou J, Liu Z, Li F. Upconversion nanophosphors for small-animal imaging. *Chem Soc Rev.* 2012;41(3):1323–1349. doi:10.1039/c1cs15187h
150. Liu Q, Sun Y, Li C, et al. 18F-labeled magnetic-upconversion nanophosphors via rare-earth cation-assisted ligand assembly. *ACS Nano.* 2011;5(4):3146–3157. doi:10.1021/nn200298y
151. Zou W, Visser C, Maduro JA, Pshenichnikov MS, Hummelen JC. Broadband dye-sensitized upconversion of near-infrared light. *Nat Photonics.* 2012;6:560. doi:10.1038/nphoton.2012.158
152. Zijlmans HJMAA, Bonnet J, Burton J, et al. Detection of cell and tissue surface antigens using up-converting phosphors: a new reporter technology. *Anal Biochem.* 1999;267(1):30–36. doi:10.1006/abio.1998.2965
153. Wu S, Han G, Milliron DJ, et al. Non-blinking and photostable upconverted luminescence from single lanthanide-doped nanocrystals. *Proc Natl Acad Sci.* 2009;106(27):10917–10921. doi:10.1073/pnas.0904792106
154. Vaithyanathan M, R Bajgiran K, Darapaneni P, Safa N, Dorman JA, Melvin AT. Luminescent nanomaterials for droplet tracking in a microfluidic trapping array. *Anal Bioanal Chem.* 2019;411(1):157–170. doi:10.1007/s00216-018-1448-1
155. Pominova DV, Ryabova AV, Romanishkin ID, Makarov VI, Grachev PV. Bioimaging with controlled depth using upconversion nanoparticles. Paper presented at: SPIE Photonics Europe 2018.
156. Raab O. Über die Wirkung Fluoreszierender Stoffe auf Infusorien. *Z Biol.* 1900;39:524–546.
157. Von Tappenier H. Therapeutische versuche mit fluoreszierenden stoffen. *Muench Med Wochenschr.* 1903;47:2042–2044.
158. Figue FH, Weiland GS, Manganiello LO. Cancer detection and therapy; affinity of neoplastic, embryonic, and traumatized tissues for porphyrins and metalloporphyrins. *Proc Soc Exp Biol Med Soc Exp Bio Med.* 1948;68(3):640. doi:10.3181/00379727-68-16580

159. Schwartz S, Absolon K, Vermund H. Some relationships of porphyrins, X-rays and tumors. *Univ Minn Med Bull.* 1955;27:7.
160. Kelly J, Snell M. Hematoporphyrin derivative: a possible aid in the diagnosis and therapy of carcinoma of the bladder. *J Urol.* 1976;115(2):150–151. doi:10.1016/s0022-5347(17)59108-9
161. Idris NM, Jayakumar MKG, Bansal A, Zhang Y. Upconversion nanoparticles as versatile light nanotransducers for photoactivation applications. *Chem Soc Rev.* 2015;44(6):1449–1478. doi:10.1039/c4cs00158c
162. Oleinick NL, Morris RL, Belichenko I. The role of apoptosis in response to photodynamic therapy: what, where, why, and how. *Photochem Photobiol Sci.* 2002;1(1):1–21. doi:10.1039/b108586g
163. Mittal M, Siddiqui MR, Tran K, Reddy SP, Malik AB. Reactive oxygen species in inflammation and tissue injury. *Antioxid Redox Signal.* 2013;20(7):1126–1167. doi:10.1089/ars.2012.5149
164. Stummer W, Hassan A, Kempfski O, Goetz C. Photodynamic therapy within edematous brain tissue: considerations on sensitizer dose and time point of laser irradiation. *J Photochem Photobiol B.* 1996;36(2):179–181.
165. Lucky SS, Soo KC, Zhang Y. Nanoparticles in photodynamic therapy. *Chem Rev.* 2015;115(4):1990–2042. doi:10.1021/cr5004198
166. Spyratou E, Makropoulou M, Efstathopoulos E, Georgakilas A, Siver L. Recent advances in cancer therapy based on dual mode gold nanoparticles. *Cancers.* 2017;9(12):173. doi:10.3390/cancers9120173
167. Idris NM, Gnanasammandhan MK, Zhang J, Ho PC, Mahendran R, Zhang Y. In vivo photodynamic therapy using upconversion nanoparticles as remote-controlled nanotransducers. *Nat Med.* 2012;18(10):1580–1585. doi:10.1038/nm.2933
168. Wang C, Cheng L, Liu Y, et al. Imaging-guided pH-sensitive photodynamic therapy using charge reversible upconversion nanoparticles under near-infrared light. *Adv Funct Mater.* 2013;23(24):3077–3086. doi:10.1002/adfm.201202992
169. Chen Z, Chen H, Hu H, et al. Versatile synthesis strategy for carboxylic acid-functionalized upconverting nanophosphors as biological labels. *J Am Chem Soc.* 2008;130(10):3023–3029. doi:10.1021/ja076151k
170. Zhao H, Hu W, Ma H, et al. Photo-induced charge-variable conjugated polyelectrolyte brushes encapsulating upconversion nanoparticles for promoted siRNA release and collaborative photodynamic therapy under NIR light irradiation. *Adv Funct Mater.* 2017;27(44):1702592. doi:10.1002/adfm.201702592
171. Liu B, Li C, Xing B, Yang P, Lin J. Multifunctional UCNPs@PDA-ICG nanocomposites for upconversion imaging and combined photothermal/photodynamic therapy with enhanced antitumor efficacy. *J Mater Chem B.* 2016;4(28):4884–4894. doi:10.1039/C6TB00799F
172. Zhou L, Wang R, Yao C, et al. Single-band upconversion nanoprobes for multiplexed simultaneous in situ molecular mapping of cancer biomarkers. *Nat Commun.* 2015;6:6938. doi:10.1038/ncomms7938
173. Min Y, Li J, Liu F, Yeow EKL, Xing B. Near-infrared light-mediated photoactivation of a platinum antitumor prodrug and simultaneous cellular apoptosis imaging by upconversion-luminescent nanoparticles. *Angew Chem Int Ed.* 2014;53(4):1012–1016. doi:10.1002/anie.201308834
174. Yang Y, Liu F, Liu X, Xing B. NIR light controlled photorelease of siRNA and its targeted intracellular delivery based on upconversion nanoparticles. *Nanoscale.* 2013;5(1):231–238. doi:10.1039/c2nr32835f
175. Wang M, Mi -C-C, Wang W-X, et al. Immunolabeling and NIR-excited fluorescent imaging of HeLa cells by using NaYF<sub>4</sub>: Yb, ErUpconversion nanoparticles. *ACS Nano.* 2009;3(6):1580–1586. doi:10.1021/nn900491j
176. Xiong L, Chen Z, Tian Q, Cao T, Xu C, Li F. High contrast upconversion luminescence targeted imaging in vivo using peptide-labeled nanophosphors. *Anal Chem.* 2009;81(21):8687–8694. doi:10.1021/ac901960d
177. Wang C, Cheng L, Liu Z. Drug delivery with upconversion nanoparticles for multi-functional targeted cancer cell imaging and therapy. *Biomaterials.* 2011;32(4):1110–1120. doi:10.1016/j.biomaterials.2010.09.069
178. Cardoso MM, Peca IN, Roque ACA. Antibody-conjugated nanoparticles for therapeutic applications. *Curr Med Chem.* 2012;19(19):3103–3127.
179. Feng W, Zhu X, Li F. Recent advances in the optimization and functionalization of upconversion nanomaterials for in vivo bioapplications. *NPG Asia Mater.* 2013;5:e75. doi:10.1038/am.2013.63
180. Tsoi KM, MacParland SA, Ma X-Z, et al. Mechanism of hard-nanomaterial clearance by the liver. *Nat Mater.* 2016;15:1212. doi:10.1038/nmat4718
181. Liu J, Yu M, Zhou C, Zheng J. Renal clearable inorganic nanoparticles: a new frontier of bionanotechnology. *Mater Today.* 2013;16(12):477–486. doi:10.1016/j.mattod.2013.11.003
182. Soo Choi H, Liu W, Misra P, et al. Renal clearance of quantum dots. *Nat Biotechnol.* 2007;25:1165. doi:10.1038/nbt1276
183. Liu C, Gao Z, Zeng J, et al. Magnetic/upconversion fluorescent NaGdF<sub>4</sub>: Yb,ErNanoparticle-based dual-modal molecular probes for imaging tiny tumors in vivo. *ACS Nano.* 2013;7(8):7227–7240. doi:10.1021/nn4030898
184. Ai X, Ho CJH, Aw J, et al. In vivo covalent cross-linking of photon-converted rare-earth nanostructures for tumour localization and theranostics. *Nat Commun.* 2016;7:10432. doi:10.1038/ncomms10432
185. Dai Y, Xiao H, Liu J, et al. In vivo multimodality imaging and cancer therapy by near-infrared light-triggered trans-platinum prodrug-conjugated upconversion nanoparticles. *J Am Chem Soc.* 2013;135(50):18920–18929. doi:10.1021/ja410028q
186. Dai Y, Yang D, Yu D, et al. Mussel-inspired polydopamine-coated lanthanide nanoparticles for NIR-II/CT dual imaging and photothermal therapy. *ACS Appl Mater Interfaces.* 2017;9(32):26674–26683. doi:10.1021/acsami.7b06109
187. Chen S, Weitemier AZ, Zeng X, et al. Near-infrared deep brain stimulation via upconversion nanoparticle-mediated optogenetics. *Science.* 2018;359(6376):679. doi:10.1126/science.aag1144
188. Hososhima S, Yuasa H, Ishizuka T, et al. Near-infrared (NIR) upconversion optogenetics. *Sci Rep.* 2015;5:16533. doi:10.1038/srep16533
189. Shah S, Liu J-J, Pasquale N, et al. Hybrid upconversion nanomaterials for optogenetic neuronal control. *Nanoscale.* 2015;7(40):16571–16577. doi:10.1039/c5nr03411f
190. Wu X, Zhang Y, Takle K, et al. Dye-sensitized core/active shell upconversion nanoparticles for optogenetics and bioimaging applications. *ACS Nano.* 2016;10(1):1060–1066. doi:10.1021/acsnano.5b06383
191. Akshaya B, Haichun L, Gnanasammandhan JMK, Stefan AE, Yong Z. Quasi-continuous wave near-infrared excitation of upconversion nanoparticles for optogenetic manipulation of *C. elegans*. *Small.* 2016;12(13):1732–1743. doi:10.1002/smll.201503792
192. Xiangzhao A, Linna L, Yang Z, et al. Remote regulation of membrane channel activity by site-specific localization of lanthanide-doped upconversion nanocrystals. *Angew Chem Int Ed.* 2017;56(11):3031–3035. doi:10.1002/anie.201612142

**International Journal of Nanomedicine**

Dovepress

**Publish your work in this journal**

The International Journal of Nanomedicine is an international, peer-reviewed journal focusing on the application of nanotechnology in diagnostics, therapeutics, and drug delivery systems throughout the biomedical field. This journal is indexed on PubMed Central, MedLine, CAS, SciSearch<sup>®</sup>, Current Contents<sup>®</sup>/Clinical Medicine,

Journal Citation Reports/Science Edition, EMBase, Scopus and the Elsevier Bibliographic databases. The manuscript management system is completely online and includes a very quick and fair peer-review system, which is all easy to use. Visit <http://www.dovepress.com/testimonials.php> to read real quotes from published authors.

Submit your manuscript here: <https://www.dovepress.com/international-journal-of-nanomedicine-journal>